Origin and evolution of Sariñena Lake (central Ebro Basin): A piping-based model

Carmen Castañeda, F. Javier Gracia, Rafael Rodríguez-Ochoa, Mario Zarroca, Carles Roqué, Rogelio Linares, Gloria Desir

PII: S0169-555X(17)30163-0
DOI: doi: 10.1016/j.geomorph.2017.04.013
Reference: GEOMOR 5994

To appear in: *Geomorphology*

Received date: 21 February 2017
Revised date: 30 March 2017
Accepted date: 10 April 2017

Please cite this article as: Carmen Castañeda, F. Javier Gracia, Rafael Rodríguez-Ochoa, Mario Zarroca, Carles Roqué, Rogelio Linares, Gloria Desir , Origin and evolution of Sariñena Lake (central Ebro Basin): A piping-based model. The address for the corresponding author was captured as affiliation for all authors. Please check if appropriate. Geomor(2017), doi: 10.1016/j.geomorph.2017.04.013

Origin and evolution of Sariñena Lake (central Ebro Basin): a piping-based model

Carmen Castañeda[a]*, F. Javier Gracia[b], Rafael Rodríguez-Ochoa[c], Mario Zarroca[d1], Carles Roqué[e], Rogelio Linares[d], Gloria Desir[f]

[a]Estación Experimental de Aula Dei, EEAD-CSIC, Zaragoza, Spain

[b]Departamento de Ciencias de la Tierra, Universidad de Cádiz, Cádiz, Spain

[c]Departamento de Medio Ambiente y Ciencias del Suelo, Universidad de Lleida, Lleida, Spain

[d]Departamento de Geología, Universidad Autónoma de Barcelona, Barcelona, Spain

[e]Área de Geodinámica Externa y Geomorfología, Universidad de Girona, Girona, Spain

[f]Departamento de Ciencias de la Tierra, Universidad de Zaragoza, Zaragoza, Spain

*Corresponding autor. E-mail address: ccastaneda@eead.csic.es (C. Castañeda).

[1]Serra Húnter fellow.

Abstract

The origin and nature of the numerous lakes in the central Ebro Basin have been interpreted according to the prevailing arid or semiarid conditions, the easily-eroded materials and the solubility of the gypsum- and/or carbonate-rich Tertiary/Cenozoic substratum, involving important dissolution (karstic) and/or aeolian deflation. However, the origin of Sariñena Lake, the largest in the central Ebro Basin, remains unknown since the typical lake-generating processes in the region are not applicable. This work provides significant clues to the genesis and evolution of Sariñena Lake in a regional context. The combination of geomorphological mapping and high resolution LiDAR

data together with sedimentological observations, the characterisation of soils and sediments around the lake, and the application of high-resolution geophysical techniques suggests that piping is the major genetic process driving the evolution of the Sariñena depression and lake. Field evidence demonstrates that piping is, at present, the most important erosive process in the region, generating significant collapse and surface lowering. Sariñena Lake is located within a deep endorheic depression excavated from Na-rich Tertiary materials. This work hypothesises that once an early, fluvially-originated palustrine area had developed, the progressive lowering of the regional water table linked to regional fluvial incision favoured the establishment of a hydrological gradient high enough to trigger piping processes within the claystones and siltstones underlying the original palustrine area. The Quaternary evolution of the Sariñena lacustrine basin was then controlled by successive water table fluctuations, linked to different phases of incision and alluvial deposition in the surrounding fluvial systems. All the evidence supporting a piping-related origin for this lake, together with examples of lakes generated by similar processes in different contexts, is used to propose a new genetic type of lacustrine depression, generated by piping processes under favourable conditions.

Keywords: Ebro Depression; Lake geomorphology; Northeast Spain; Sodic soils;

1. Introduction

Establishing the origin of a given lake is not always easy because very often different geological or geomorphological processes interact to produce closed depressions where water subsequently accumulates, and these processes evolve over time. Major processes in lacustrine basin formation are generally regionally controlled (Reeves, 1968) and

hence regional factors like climate, geology, geomorphological context, and evolution must be explored in detail. Lakes of complex origin (Wright, 1964; Wood and Osterkamp, 1987) are very often difficult to ascribe to a specific genetic type using traditional (Hutchinson, 1957; Timms, 1992; Hakanson, 2007) or other integrative classifications (Semeniuk and Semeniuk, 1995). In such cases, applying a single criterion to genetically classify a lake seems too simplistic and may lead to misinterpretation. This difficulty can be resolved by employing different methods that infer the geometry of the basin, the relationship between the basin and its substrata, the possible processes responsible for generating the depression, and its subsequent evolution. This work illustrates the application of different methods to the genetic and evolutionary interpretation of Sariñena Lake (Ebro Basin, NE Spain, Fig. 1), the origin of which is rather controversial.

The Tertiary Ebro Basin is one of the most important basins on the Iberian Peninsula, located to the south of the Pyrenean Range, north of the Iberian Range, and west of the Catalan Coastal Range. Although drained along its axis by the Ebro River, various environmental factors, such as the prevailing semiarid climate, very low relief in the area, and predominant outcrops of impervious materials, favour the generation of endorheic areas, usually occupied by small, ephemeral lakes. The literature on the origin and nature of the numerous lakes in the Ebro Basin is abundant and dates back to the beginning of the 20th century (Aramburu, 1904; Dantin, 1942; Quirantes, 1965; Ibáñez, 1975; Mingarro et al., 1981; Alberto et al., 1984; Sánchez et al., 1998; Gutiérrez et al., 2002a, among other authors). Most lacustrine depressions in the central zone of the basin are small, very shallow, and involve groups of lakes developed on wide morphostructural platforms or alluvial plains. Sariñena Lake, however, does not share these characteristics.

Ibáñez et al. (1984) recognised the difficulty of interpreting the origin and evolution of Sariñena Lake. These authors presented a summary of the factors favouring the maintenance of endorheic zones in the Ebro Basin, including those cited above, and concluded that this lacustrine basin probably formed as a combination of processes: differential weathering and erosion during humid periods, and aeolian deflation during dry periods. This hypothesis is in stark contrast with the notable depth of the lacustrine depression and the steep slopes surrounding the lake. Moreover, aeolian sediments are very scarce and local in the area (Desir et al., 2011), indicating a limited deflational effect, the most important traces of which can be recognised in the form of some rocky yardangs (Gutiérrez et al., 2002a), ventifacts (Cuchí et al., 2012), and small local dunes (Sancho et al., 2004).

Hernández Samaniego et al. (1998) considered a possible karstic origin for the lake, given the frequent calcareous clasts in the Pleistocene fluvial deposits surrounding it, which could have dissolved to produce a doline-like depression. However, this hypothesis is difficult to support as the lime-rich deposits are only a few metres thick and the present-day lake, and most of the lacustrine depression, is predominantly excavated from non-soluble materials: claystones, siltstones, and quartz-sandstones. A third hypothesis once again refers to the possible dissolution of gypsarenites present as channels in the Tertiary units underlying the terrace on which the Sariñena Lake depression is developed (Hernández Samaniego et al., 1998), despite the relative scarcity of this type of sediment in the lake surroundings (Costa et al., 1998; Hernández Samaniego et al., 1998).

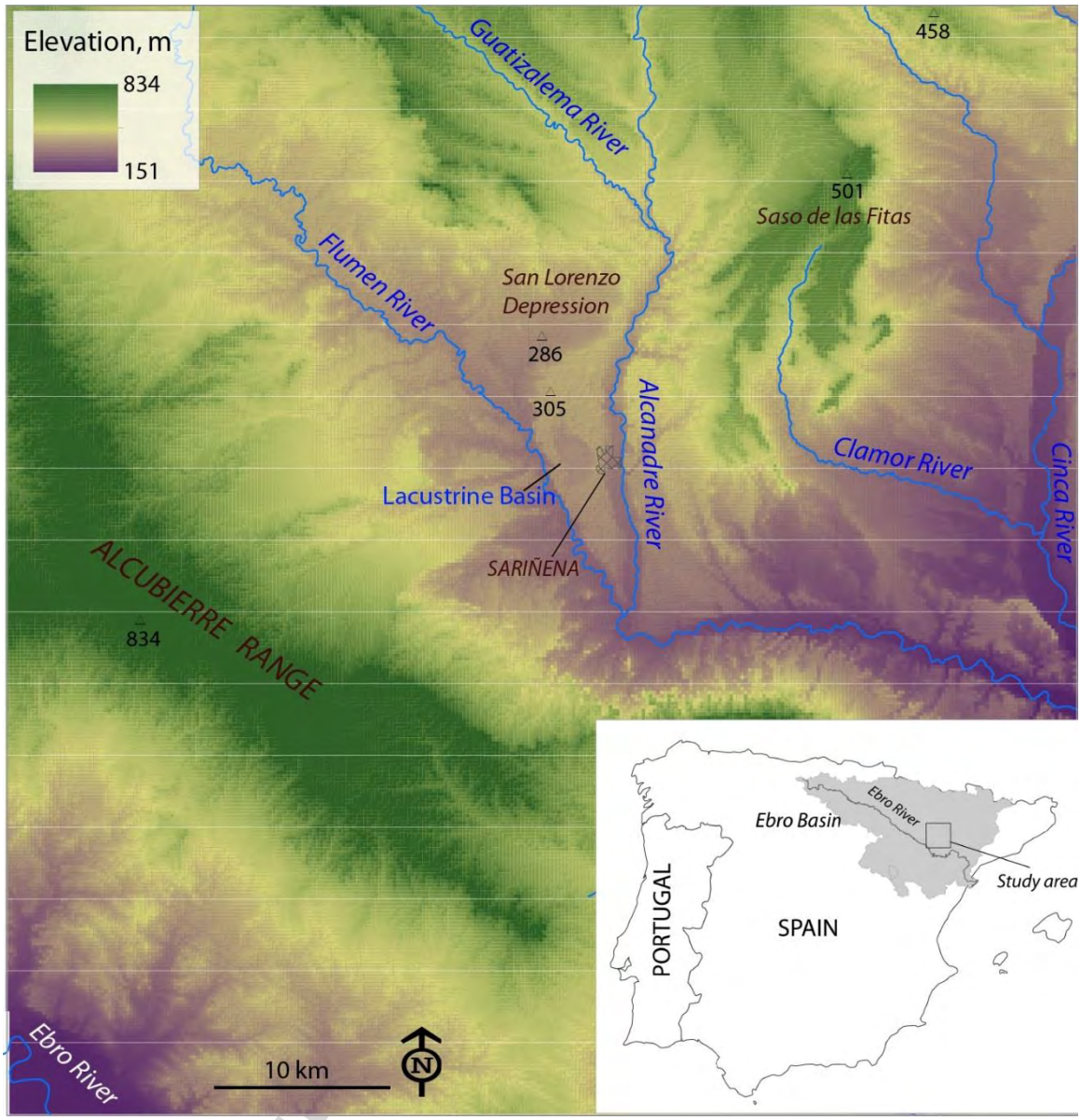

Fig. 1. Elevation of the Sariñena high plain in the central Ebro Basin. Digital elevation model (pixel = 200 m) obtained from www.ign.es/ in ASCII grid ARC/INFO format derived from interpolation of 5-m pixel DEM.

Sariñena is an example of where the normal lake-generating processes prevailing in the region do not apply. Once the genetic origins suggested by the abovementioned authors have been ruled out, it is possible to propose a new model of lake generation for Sariñena Lake involving soil and sediment piping processes. This work utilises a multidisciplinary approach to reconstruct the origin and evolution of the lake. High-

resolution topographic data together with stereo photointerpretation and sedimentological observations of the substratum outcrops surrounding the lake provide important clues as to the timing and general causes of onset of the initial endorheic conditions. The physical and chemical characterisation of soils and sediments surrounding the lake give information about the possible processes conducive to the genesis of the lake. Electrical resistivity imaging (ERI) and complementary seismic refraction tomography (SRT) were applied in the zone in order to recognise possible piping structures within the basin. The study shows how integrating data collected through complementary techniques may provide significant information on the genesis and evolution of lakes.

2. Geological and geomorphological setting

The central zone of the Ebro Basin comprises a sequence of horizontal Neogene sedimentary materials of various lithologies, ranging from conglomerates and sandstones in the vicinity of the Pyrenean Range, clays, marls, and gypsum in the intermediate area, to Middle-Late Miocene lacustrine limestones in the centre of the basin (Quirantes, 1978; Riba et al., 1983; Arenas and Pardo, 1999; Luzón et al., 2002).

The study zone is in the intermediate area (Fig. 2) where the substrata are mainly yellow claystones and siltstones with occasional 0.1-2 m-thick sandstone lenses of Middle Miocene age (Agenian to Aragonian, according to Costa et al., 1998, and Hernández Samaniego et al., 1998). Sedimentological details of these units can be found in Luzón (2005), along with their palaeogeographical significance. No significant tectonic structures have been identified in the area. Only minor fractures and E-W and N-S oriented joints affect the sandstones lenses at a local scale (Arlegui and Soriano, 1998; Costa et al., 1998).

Differential erosion of the Neogene materials in the Ebro Basin has led to the excavation of wide topographic lows. This process has been accelerated by the presence of easily eroded materials, mainly clays, silts and gypsum (Fig. 2). Fluvial excavation and rapid river migration favoured the sedimentation of extensive Quaternary morphosedimentary units whose staircase morphology and chronology point to different phases of floodplain aggradation and river incision associated with climatic variations, glacial pulses and tectonic uplift in the Pyrenees in the Mid-Late Pleistocene (Lewis et al., 2009; Stange et al., 2013, 2016).

The Quaternary deposits in the zone principally comprise stepped sequences of fluvial terraces and associated pediments descending from the surrounding relief. These were previously identified and mapped by several authors (Mensua and Ibáñez, 1977; Bomer, 1979; Alberto et al., 1984; Calle et al., 2013; Badía et al., 2015; Montes et al., 2016).

The Sariñena Lake occupies the bottom of a basin inset into a wide mesa approximately 300 m above sea level, which forms the main divide between the Alcanadre and Flumen rivers prior to their confluence (Fig. 1). The mesa is composed of Pleistocene fluvial deposits 0.5–4 m thick (Ibáñez et al., 1984) and constitutes an old perched terrace hanging more than 40 m above the nearby fluvial valleys. The mesa is elongated and extends for approximately 18 km in a N-S direction, being 4 km wide in its central sector. It is limited to the N and NE by a series of high plains, the highest reaching an altitude of about 500 m (Saso de las Fitas, Fig. 1), all of which developed in Lower Pleistocene alluvial deposits with a mean electron spin resonance (ESR) age of 1276 ± 104 ky (Duval et al., 2015), making them probably the oldest Quaternary fluvial deposits on the Iberian Peninsula (Sancho et al., 2016).

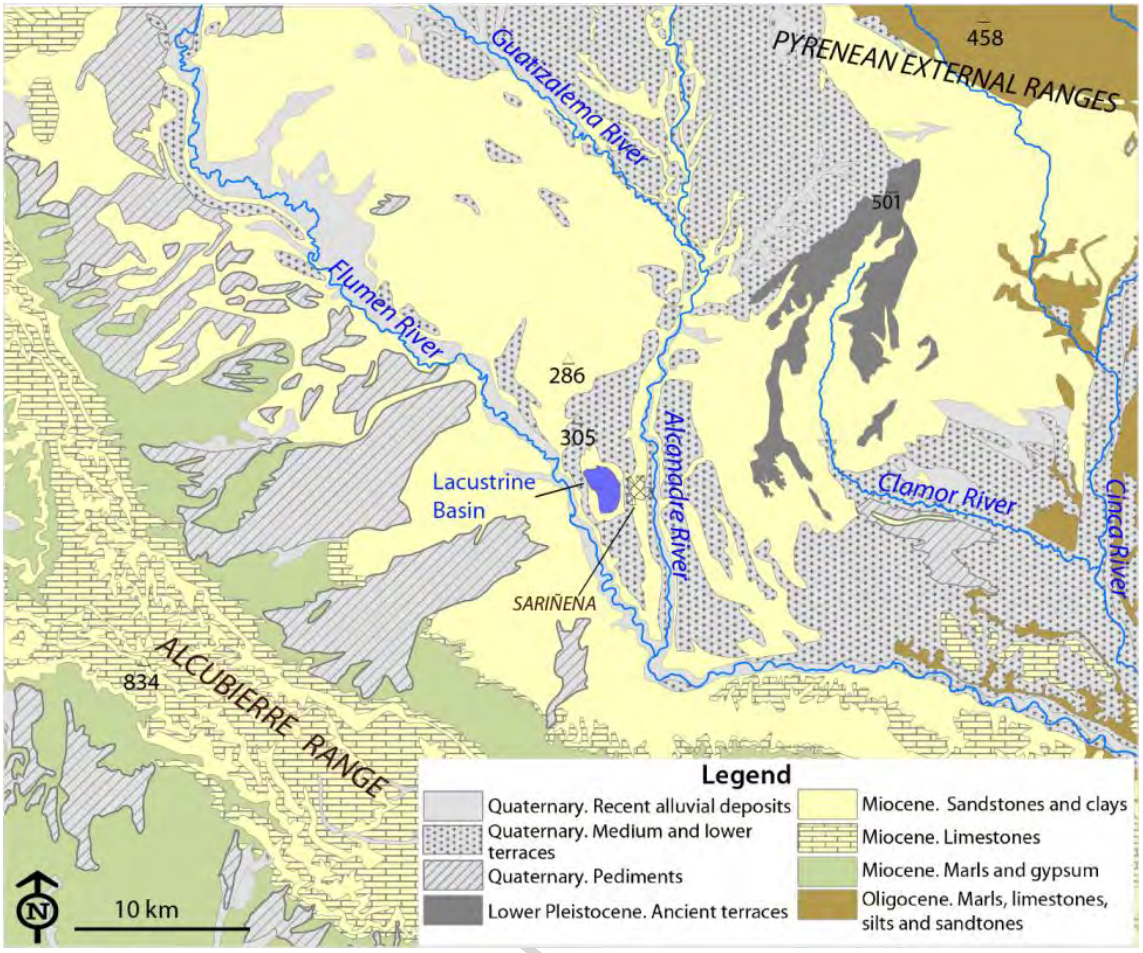

Fig. 2. Regional geological setting of the Sariñena high plain.

The Alcanadre River valley has six stepped alluvial levels according to Costa et al. (1998) and Hernández Samaniego et al. (1998), and nine according to Calle et al. (2013). Terrace level numbering differs between the authors, since the first two groups began counting the levels on the lowest surface while the latter took the opposite approach. The relative heights of the terraces estimated in these studies are shown in Tables 1 and 2. OSL and palaeomagnetic dating of samples taken from different terrace levels allowed the age of the alluvial sequence to be estimated (Table 2). The thickness of all these fluvial deposits decreases with age (Calle et al., 2013). They comprise different polymictic gravel and sand levels, capped by typical floodplain silts and clays.

Table 1. Pediment and fluvial terrace levels in the Alcanadre, Flumen and Cinca rivers (Costa et al., 1998; Hernández Samaniego et al., 1998).

Pediment levels	Alcanadre River	Flumen River	Cinca River
	Pyrenean piedmont high level (+ 180 m)		
P5	T6 (+ 60-100 m)		
P4	T5 (+ 65-70 m)		
P3	T4 (+ 35-60 m)	T3 (+ 35-40 m)	T3 (+ 30-40 m)
P2	T3 (+ 20-30 m)	T2 (+ 20-25 m)	
P1	T2 (+ 15 m)		T2 (+ 15 m)
	T1 (+ 10 m)	T1 (+ 10 m)	T1 (+ 10 m)

Table 2. The Alcanadre River terrace levels and their estimated ages (Calle et al., 2013).

Terrace level	Absolute height m a.s.l.	Relative height m	Estimated age kyr
T1	420	160-200	1276
T2	---	100	1000 – 780
T3	325	55	780
T4	300	30	< 780
T5	270	20-25	44
T6	---	25	19
T7	260	10	10
T8	255	3-5	---
T9	250	Present floodplain	

The climate in the area is typically semiarid with a mean annual rainfall of 407 mm and 1306 mm of annual evapotranspiration measured at the neighbouring Grañén weather station (Faci and Martínez-Cob, 1991). The area is moderately windy and strong winds in winter are coming from the NW a 13% of the time (Martínez-Cob et al., 2010). The hydric regime of the present Sariñena Lake does not respond to the semiarid climatic conditions of the area but shows strong evidence of the impact of irrigation return flows. The formerly small lake (~100 ha) (Figs. 3A and B), whose variable salinity has been conditioned since Roman times by historical irrigation flows, has been reshaped into a permanent freshwater lake of about 200 ha (Fig. 3C). At present, the lake is regulated up to a maximum of 2.5 m depth to prevent the lake from flooding the adjacent agricultural areas.

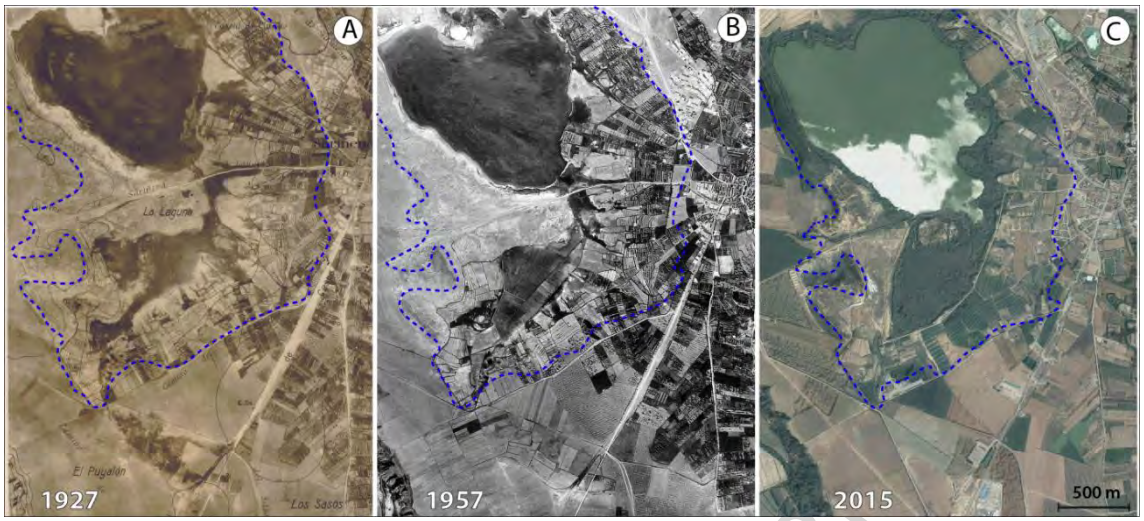

Fig. 3. Sariñena Lake: (A) 1927 photomap; (B) 1957 USAF aerial photograph; and (C) 2015 PNOA orthophotograp. The blue line broadly outlines the limits of the lacustrine depression. Note the palustrine area extending to the south of the lake.

3. Materials and methods

Geomorphological mapping was based on stereoscopic photointerpretation performed using pairs of black and white aerial photographs from 1957, from US Air Force flight B, printed at 1:33,000 scale. Other complementary aerial photographs were also used; these dated from 1927, at 1:40,000 scale supplied by the Ebro Basin Water Authority, to a PNOA (National Programme for Aerial Orthophotography) flight from 2015, with 0.5 m pixels.

The resulting geomorphological map and the 1957 aerial photographs were scanned, georeferenced, and transferred directly onto the screen using ArcGIS® 10.3. A digital elevation model (DEM) generated in 2010 from airborne LiDAR data (PNOA project) was used to refine the photointerpretation and determine the height of the fluvial terraces. The DEM has an absolute vertical accuracy of 0.20 m and a density of 0.5 points/m^2. Absolute and relative heights were measured from a series of topographic profiles drawn from N to S through the Sariñena high plain. A complementary DEM

(GIS Oleícola), generated in 1997 with 20 m pixels, was also used to provide a comprehensive topography of the entire high plain. Topographic maps at 1:25,000 scale were overlain to refine and reshape the current outlines of rivers and floodplains. A subsequent field survey was carried out in the lake basin and at selected sites across the high plain and in the surrounding areas, in order to identify different landforms and processes.

Soils representative of the geomorphic units within the Sariñena Basin and complementary soils and sediments from the whole area were studied. Soil profiles were described following Schoeneberger et al. (2012) and SINEDARES (CBDSA, 1983). Genetic and diagnostic horizons and soil classification was based on Soil Taxonomy (Soil Survey Staff, 2014). The soil samples were air dried and sieved to < 2 mm for subsequent laboratory analyses. Soil salinity was measured as the electrical conductivity of the 1:5 soil:water extract and the aqueous extract of saturated paste (United States Salinity Laboratory Staff, 1954) using a conductivity cell (Orion 013605MD) and expressed in dS m^{-1} at 25 °C; pH of the 1:2.5 soil:water extract of the soil was measured using a pH electrode (Orion 9157BNMD). Calcium carbonate equivalent was measured with gasometry (MAPA, 1994), and the gypsum content was determined using thermogravimetry (Artieda et al., 2006) and confirmed with the qualitative test (Van Reeuwijk, 2002) for gypsum content < 2%. The ionic content (Na, Ca and Mg) of saturated paste extracts was analysed using an ionic chromatograph (Metrohm 861 Advanced compact IC) (APHA, 1989). Organic matter content was determined by chromic acid digestion (Heanes, 1984) and a UV/V UNICAM8625 spectrophotometer; particle size distribution was assessed by laser diffraction with a correction for the clay value following Taubner et al. (2009). The sodium adsorption ratio (SAR) was used as a measure of the relative concentrations of Na^+ versus Ca^{2+}

plus Mg^{2+}. Clay mineralogy was studied through X-ray powder diffraction (XRD) using a Bruker D8 ADVANCE diffractometer with graphite-monochromated CuK(a) radiation and a linear VANTEC detector. XRD patterns were obtained from random powder mounts and oriented mounts.

In September 2016, a geophysical survey was conducted in two selected areas: south of Laguneta and north of Puyalón (Fig. 4), where surface features suggested the possible presence of piping structures presumably associated with the genesis of the lake. Electrical resistivity imaging (ERI) profiles were collected using a Lund Imaging system comprising 64 electrodes according to the Dipole-Dipole (DDP) array. DDP was selected because it provides dense data coverage and good horizontal resolution, valuable for identifying sharp lateral variations caused by vertical structures (Dahlin and Zhou, 2004).

ERI has been demonstrated to be particularly effective for detecting piping structures developed in landslide deposits (Giampaolo et al., 2016), pseudokarstic features in loess deposits (Zeng et al., 2016), anthropogenic cavities (Martínez-Pagán, et al., 2013), and piping voids affecting earth dams (Loperte et al., 2016). The Laguneta profile was 80 m long with an inter-electrode spacing of 1-2 m (1 m for the inner electrodes and 2 m for the outer ones) to gain resolution. The Puyalón profile was 400 m long with an inter-electrode spacing of 5-10 m in order to investigate deeper features of the piping system, even though this was detrimental to the resolution. The apparent resistivity records were inverted by the EarthImager2D software (Advanced Geosciences, Inc). Despite the gentle topographic curve, topographic correction of the model was carried out using the LiDAR-based DEM. A seismic refraction tomography (SRT) profile was acquired overlapping the ERI profile at the Laguneta site, with the aim of better constraining the higher-resolution resistivity image. The seismic P-velocities were recorded using a 12-

channel seismograph ES-1225 (EG&G Geometrics), 12 geophones of 10 Hz, spaced at 5 m intervals (with the exception of the terminal geophones that were placed at 2.5 m), and a 5 kg sledge hammer that acted as the energy source. The seismic inversion was performed with the SeisImager2D software suite (EG&G Geometrics).

4. Results

4.1. Sariñena high plain and main landforms

Up to seven fluvial terrace levels, in addition to the present floodplain, have been recognised in the Alcanadre River valley in the vicinity of the Sariñena mesa (Table 3 and Fig. 4). The higher levels, T6 and T7, are mainly represented on the eastern side of the valley, although some isolated remnants of these old levels can be recognised along the northern and western sides of the Sariñena mesa (Figs. 4 and 5A), resting on the T5 level. The Sariñena high plain corresponds to level T5. The photointerpretation and LiDAR-derived topography show an apparent split in T5 evidenced by the occurrence of a subtle to noticeable escarpment paralleling the eastern border of the Sariñena high plain. The lowest terrace levels, from T4 to T1, are asymmetrically distributed on the two sides of the present-day Alcanadre River valley (Fig. 5) with notable N-S elongation and very limited E-W extension.

The Flumen River valley is much more asymmetrical, with a complete sequence of staircased terrace and pediment levels on the SW margin and a very steep erosional escarpment through Miocene claystones and sandstones on the NE side (Fig. 2), presumably as a consequence of the lateral migration of the river course towards the NE.

The Sariñena high plain is topographically almost flat, with a very gentle slope of 0.4-0.5% towards the S (Fig. 4 inset). The basin divides the plain into two areas, a northern

area with a fan-like shape open towards the SW, and a southern area with a more triangular and elongated form, sloping to the S. Despite the systematic levelling caused by decades of agricultural transformation over much of the area, the LiDAR-derived topographic profiles highlight the convex shape of terrace T5 (Fig. 5) and its persistent decline towards the W, especially in the northern area (Fig. 4 inset).

Table 3. LiDAR-derived height of the fluvial terrace levels (T) in the Alcanadre-Flumen River system and the lacustrine pediment-terraces (PT) of the Sariñena Basin.

Terraces in Alcanadre-Flumen River system				**Pediment-terraces in Sariñena basin**		
Level	Relative* height	Height range	Standard deviation	Level	Height above the lake bottom	Height above the Alcanadre River thalweg
	m				m	
T7	63.1	27.4	10.7			
T6	45.1	3.8	1.7			
T5	40.9	11.8	4.3	PT3	9-13	33-37
T4	32.9	9.6	4.4	PT2	4-7	28-31
T3	25.1	10.8	3.9	PT1	2-3	24-27
T2	13.9	4.9	1.6			
T1	8.6	4.7	2.0			

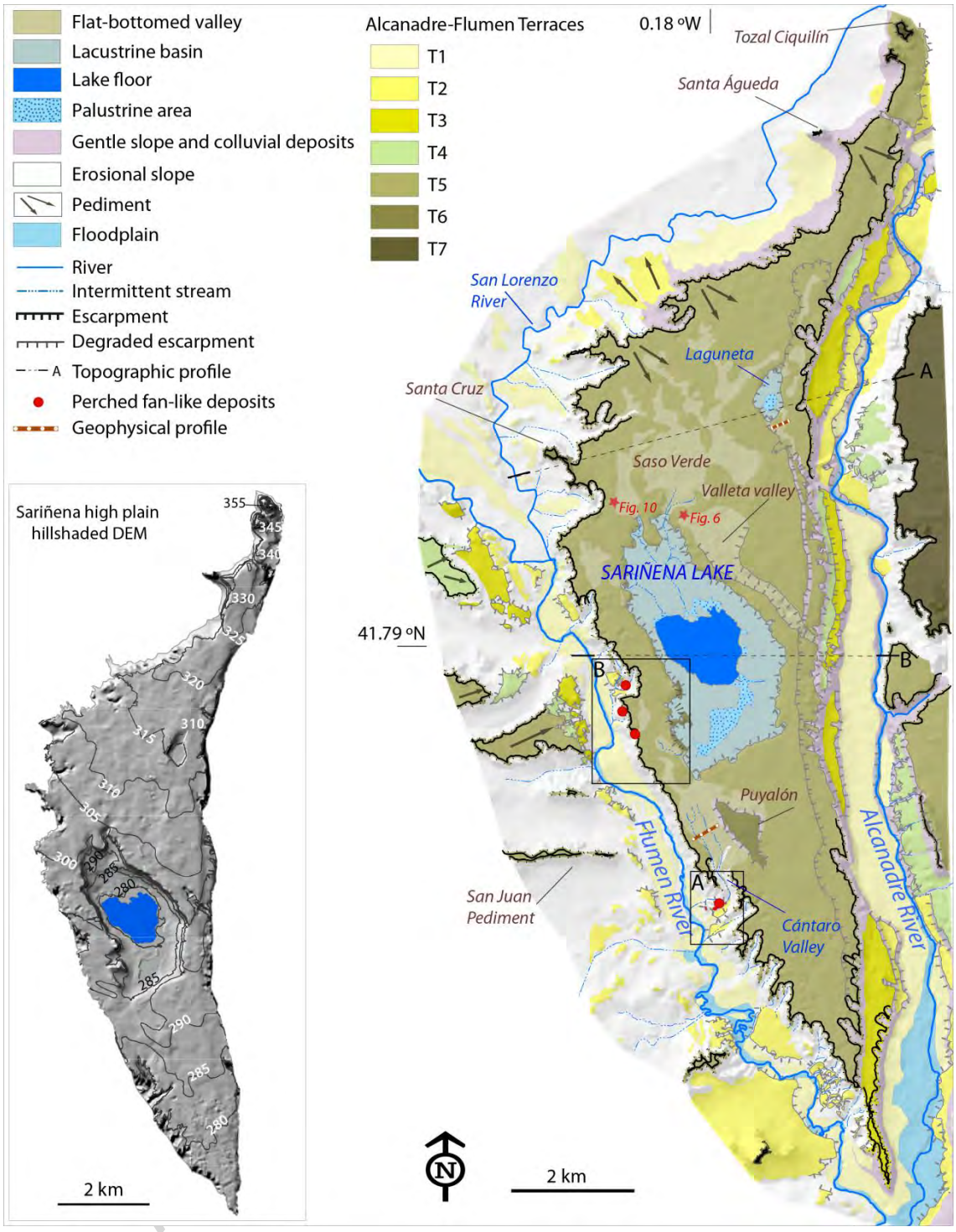

Fig. 4. Geomorphological map of the Sariñena high plain showing the locations of the topographic profiles in Fig. 5, and frames A and B illustrated in detail in Fig. 11. The inset shows the topography of the Sariñena high plain with 5 m-spaced contour lines overlying the hill-shaded GIS Oleícola DEM.

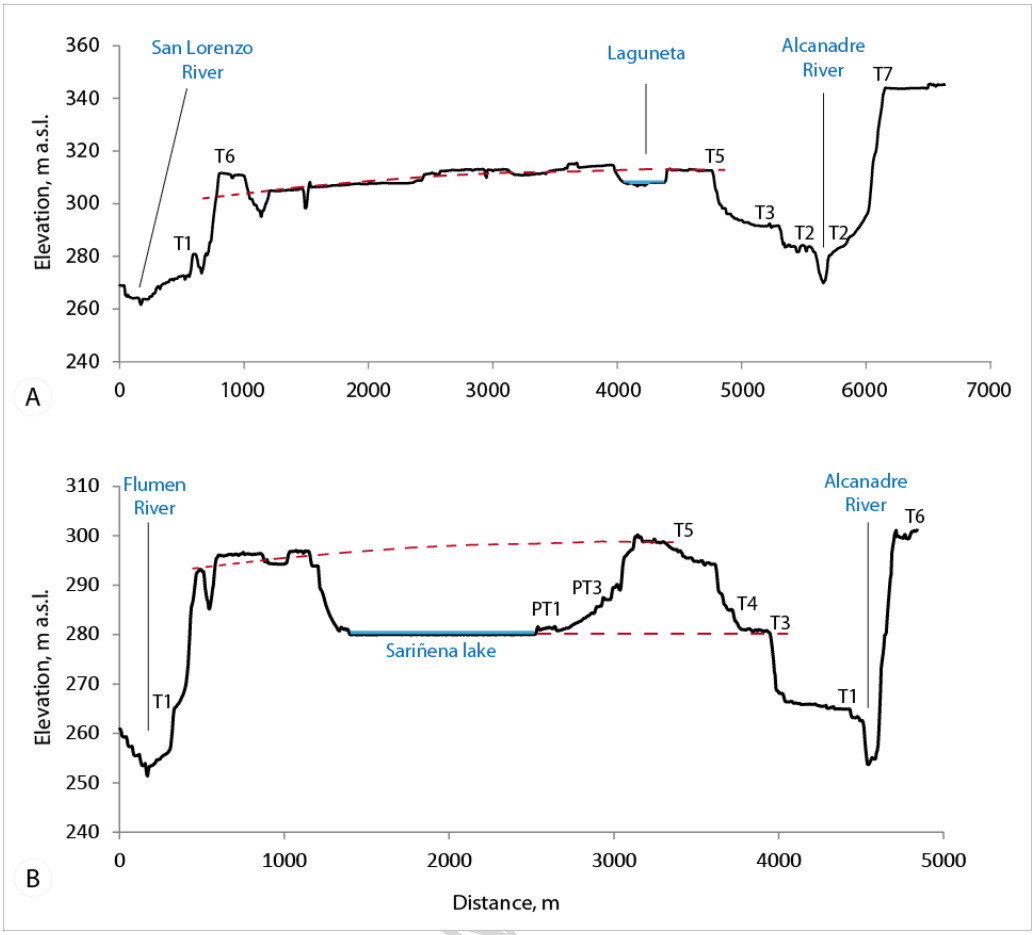

Fig. 5. LiDAR-derived topographic cross sections of the Sariñena high plain. Location shown in Fig. 4.

The fluvial deposits from the Flumen and Alcanadre Rivers are broadly similar in composition, although several diagnostic differences can be used to distinguish them. Flumen River deposits contain low centile (< 10 cm) and median (~ 3 cm) clast sizes and frequent subangular fragments of Miocene limestone supplied by the pediments derived from the Alcubierre Range (Fig. 2). Alcanadre River deposits present higher centile (> 20 cm) and median (~ 5 cm) clast sizes and virtually no Miocene limestone fragments. The difference in grain size between the two fluvial deposits was analysed and quantified by Ibáñez et al. (1984).

There are also sedimentological differences between the deposits associated with the higher (T5-T7) and lower (T1-T4) terrace levels. Higher deposits, regardless of whether they are ascribed to the Flumen or Alcanadre rivers, show a certain degree of rubefaction and most gravels present typical carbonate coatings, indicating iron oxide segregation and carbonate washing processes. These diagnostic characteristics, already described and quantified by Badía et al. (2015) in this zone, are absent in the deposits associated with the lower levels, whose gravels are mainly grey. The development of petrocalcic horizons in the high levels (Badía et al., 2015), including T5, favoured the preservation of these features.

A railway trench cutting the high plain in a broad E-W direction has exposed the inner structure of the T5 deposit, allowing the recognition of two different alluvial units overlying the Miocene sandstones and claystones, separated by a planar erosive contact (Fig. 6). The lower alluvial unit comprises 1–2 m of rounded clast-supported polymictic gravels. The unit shows well-developed channels with high-angle cross-bedding, typical of a braided fluvial system. The upper level consists of less than 1 m of a more heterogeneous, sandier, fining-upward deposit with alternating layers of different grain sizes (sands with gravels and silts with clays). This upper unit includes a basal 0.3 m-thick reddish silt- and clay-rich layer overlain by unchannelised sets of sands and gravels with low-angle ($\leq 10^{o}$) planar cross-bedding, dipping to the W and SW, and showing great lateral continuity.

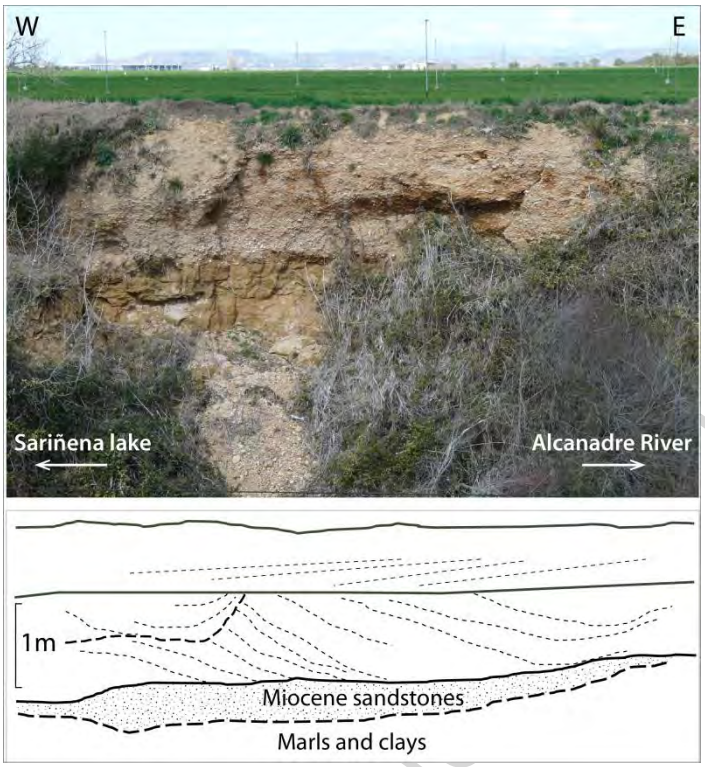

Fig. 6. General aspect of the T5 fluvial deposit in an E-W oriented railway cutting near the Sariñena depression (Location shown in Figs. 4 and 7).

The major landform of the Sariñena high plain is the Sariñena Basin (Figs. 4 and 7), located in the centre of the mesa. The basin is 540 ha in area and broadly elliptical; it measures 3.5 km in a NNW-SSE direction and 1.5 km perpendicular to this (Fig. 5B). This lacustrine basin appears as a very conspicuous hollow, inset more than 20 m into the T5 plain, with very steep margins. The southwestern and southern margins of the basin present subvertical profiles (Fig. 5B), favouring the development of small landslides (Fig. 7). The basin bottom is located at a height similar to the Alcanadre T3 level, and is inset not only into the fluvial T5 deposit but also the substratum of Miocene claystones (Fig. 5B). The height difference between the base level of Sariñena Lake and that of the Flumen River thalweg is about 20-25 m. Despite its significant lack of relief, a sequence of three stepped morphosedimentary levels have been recognised within the lacustrine basin, all of them showing a gentle centripetal slope (Fig. 7). Their

morphology and geometry are intermediate between lacustrine terraces and marginal, local pediments, so they have been denominated lacustrine pediment-terraces PT1 to PT3. They are mantled pediments with a thin veneer (< 0.5 m) of small (~3 cm) very rounded pebbles with dark coatings. The correspondence between the height of these perched lacustrine surfaces and the heights of Alcanadre-Flumen River system terraces is shown in Table 3.

The Sariñena Lake occupies the central and northern areas of the basin and is roughly triangular in form, being a maximum of 2 km long extending in a NW-SE direction, and 1.2 km in an E-W direction on its northern side (Figs. 3B and 7). According to the heights of the perched pediment-terraces surrounding the lake, the maximum water level of the lake seems never to have exceeded 289 m a.s.l. A palustrine area, subjected to intermittent flooding in the past (Figs. 3A and B), extends into the southern sector of the basin. Around the western fringe of the lake there is a narrow but continuous beach whereas incipient sand spits have developed on the southern border. These coastal forms suggest a prevailing wave-induced current moving clockwise along the shoreline (Fig. 7). Small alluvial fans are found where the occasional streams reach the lake.

A second major landform is the small lacustrine basin of Laguneta Lake (Figs. 4 and 8), located in the NE area of the plain and currently artificially drained. It is 830 m long and 450 m wide, elongated in a NNE- SSE direction, and inset about 8 m into the T5 plain (Fig. 5A). A small remnant of a perched lacustrine level can be recognised in the northern sector of the basin, about 3 m above the lake floor. The basin is outlined by a continuous sharp escarpment, with 4 m-high subvertical profiles along the eastern and southeastern borders. There is a noticeable flat-bottomed valley starting at the SE border of this depression, perched 3 m with respect to the basin bottom and less than 2 m with

respect to the T5 plain. This smooth dry valley is oriented NNW-SSE and connects the Laguneta basin border with the Alcanadre River valley (Fig. 8).

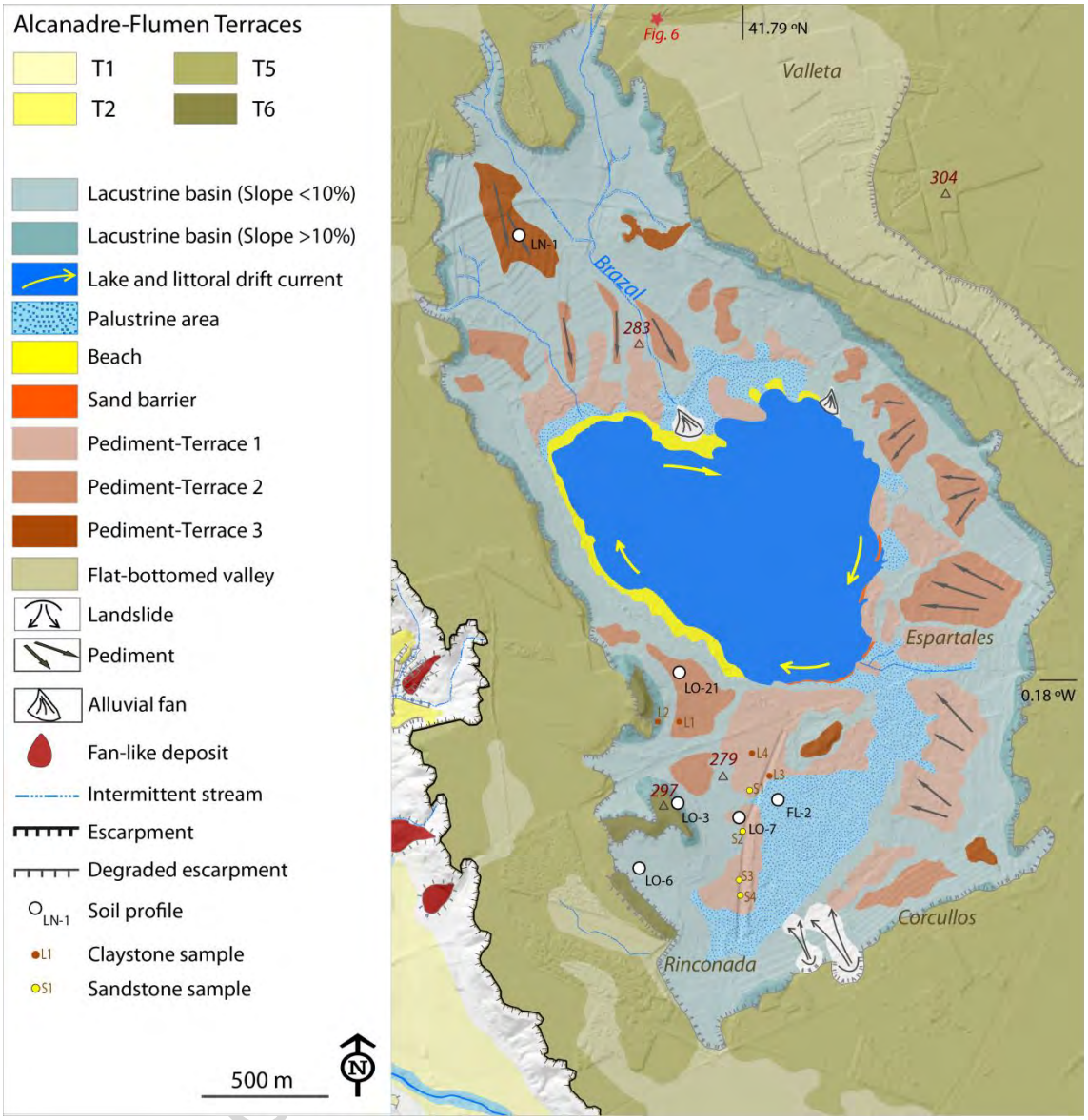

Fig. 7. Detailed geomorphological map of the Sariñena lacustrine basin overlying the LiDAR-derived hill-shaded DEM. Forms mapped according to the photointerpretation of the 1957 flight.

Flat-bottomed valleys (Fig. 4) are very common minor landforms on the T5 plain. In general, they are less than 2 m deep and follow an irregular distribution pattern. Some are partially bounded by subvertical to degraded escarpments (Fig. 7) whereas others

show little topographic evidence in the field, being obscured due to decades of agricultural land levelling and landscape transformation. Most are dry valleys with no evidence of surface streams, and they always drain towards local base levels.

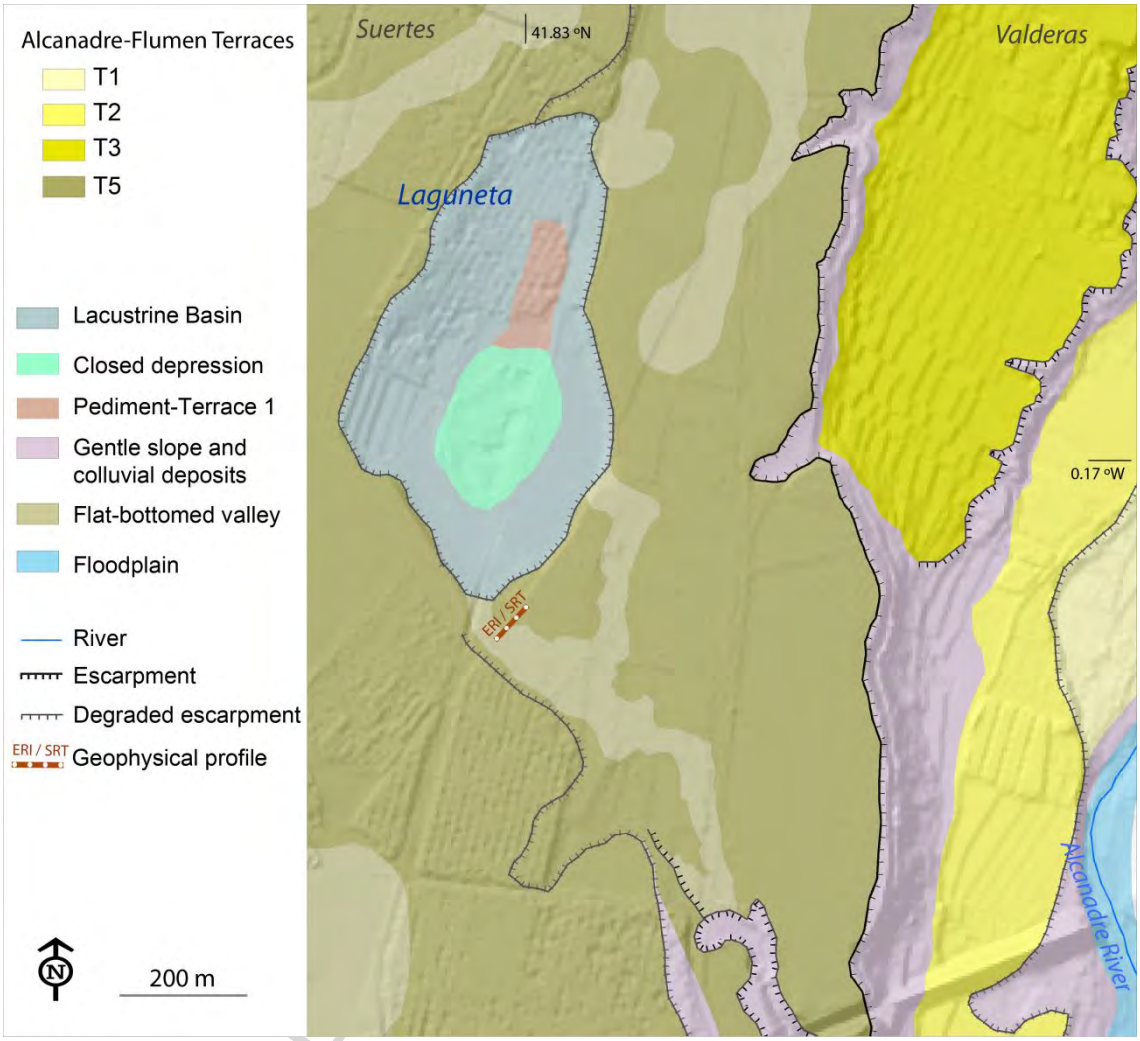

Fig. 8. Detailed geomorphological map of Laguneta Lake overlying the LiDAR-derived hill-shaded DEM.

4.2 Field evidence of piping and related structures

Field observations evidence the widespread occurrence of collapse-based erosion processes in the area. Many metric or decametric sinkholes and outlets can be seen in the Miocene outcrops, within the Sariñena basin near the lake (Figs. 9A and B), on the

surrounding slopes of the Sariñena high plain, and even at landscape scale in nearby areas (Figs. 9C and D). Soil collapse occurs in irrigated agricultural plots located on the T5 high plain. Collapse also affects the fluvial deposit of the T5 high plain. Fig. 10 illustrates an example of palaeocollapse discovered in a quarry excavated in the fluvial deposits. The structure is filled by finer reddish sediments derived from the upper floodplain layer.

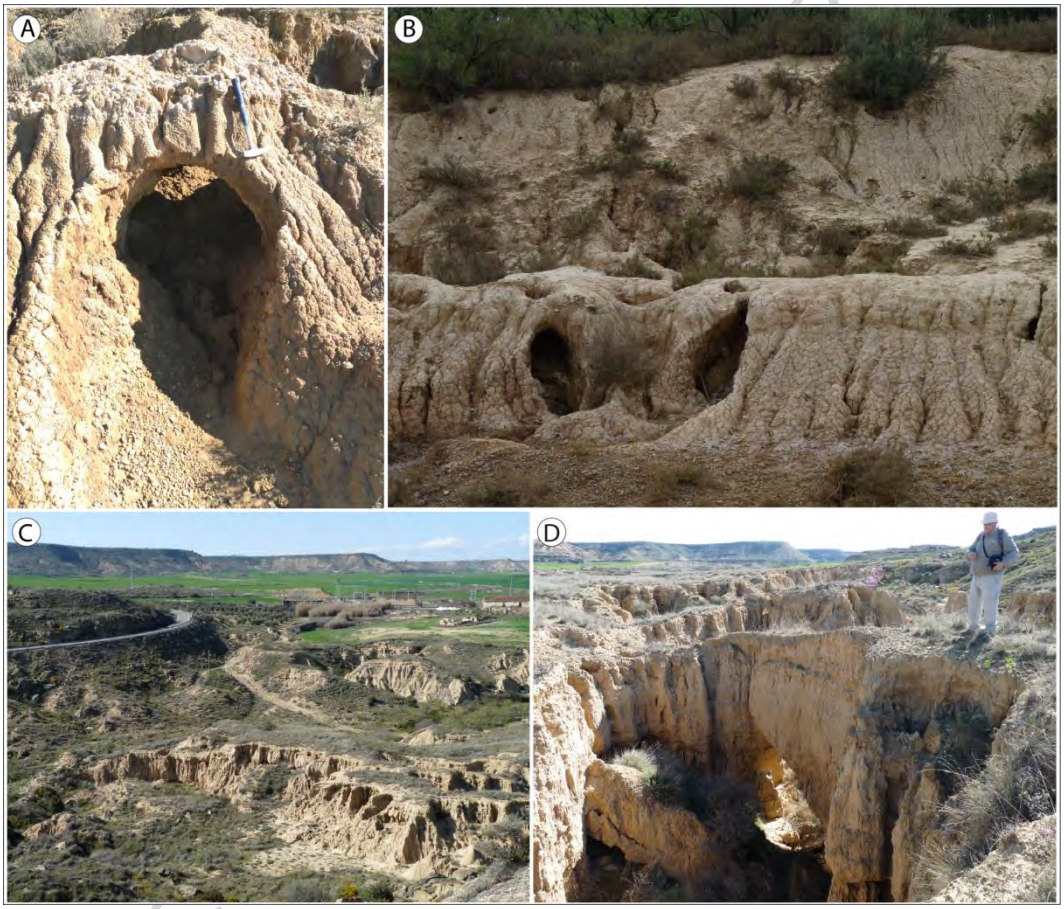

Fig. 9. (A) and (B) Pipes developed in Miocene materials and soils around Sariñena Lake. (C) and (D) Piping structures developed at landscape scale, in the nearby Clamor River valley (Location shown in Figs. 1 and 2).

Fig. 10. Collapse in terrace T5 (Location shown in Fig. 4).

Indirect indicators of past piping process activity in the zone are represented by several perched gravel-rich deposits less than 300 m in length with a characteristic fan-like form identified along the western slope of the T5 high plain (Figs. 4 and 11). The apices of all these fans are disconnected from the T5 terrace and start mid-slope, about 5-15 m below the contact between the T5 gravels and the Miocene claystones (Fig. 11). The distal edges of the fans are perched 6-11 m with respect to Flumen River (Fig. 12) corresponding in height to the T2 level. While the terrace levels show a significant lack of relief, these fans have a slope ranging from 2% in the Cántaro Valley, to 10–15% towards the Flumen River thalweg. The Cántaro Valley fan (Fig. 11A) is located at the exit of the small valley hosting the Cántaro spring, whereas the fans clustered very near Sariñena Lake (Fig. 11B) are not linked to any significant valley or gully. In contrast to the nearby Flumen terraces, all these fan deposits exclusively comprise reddish-coated gravels from the higher Alcanadre terraces, T5 to T7. The mesa slopes near the fan apices are full of pipe inlets.

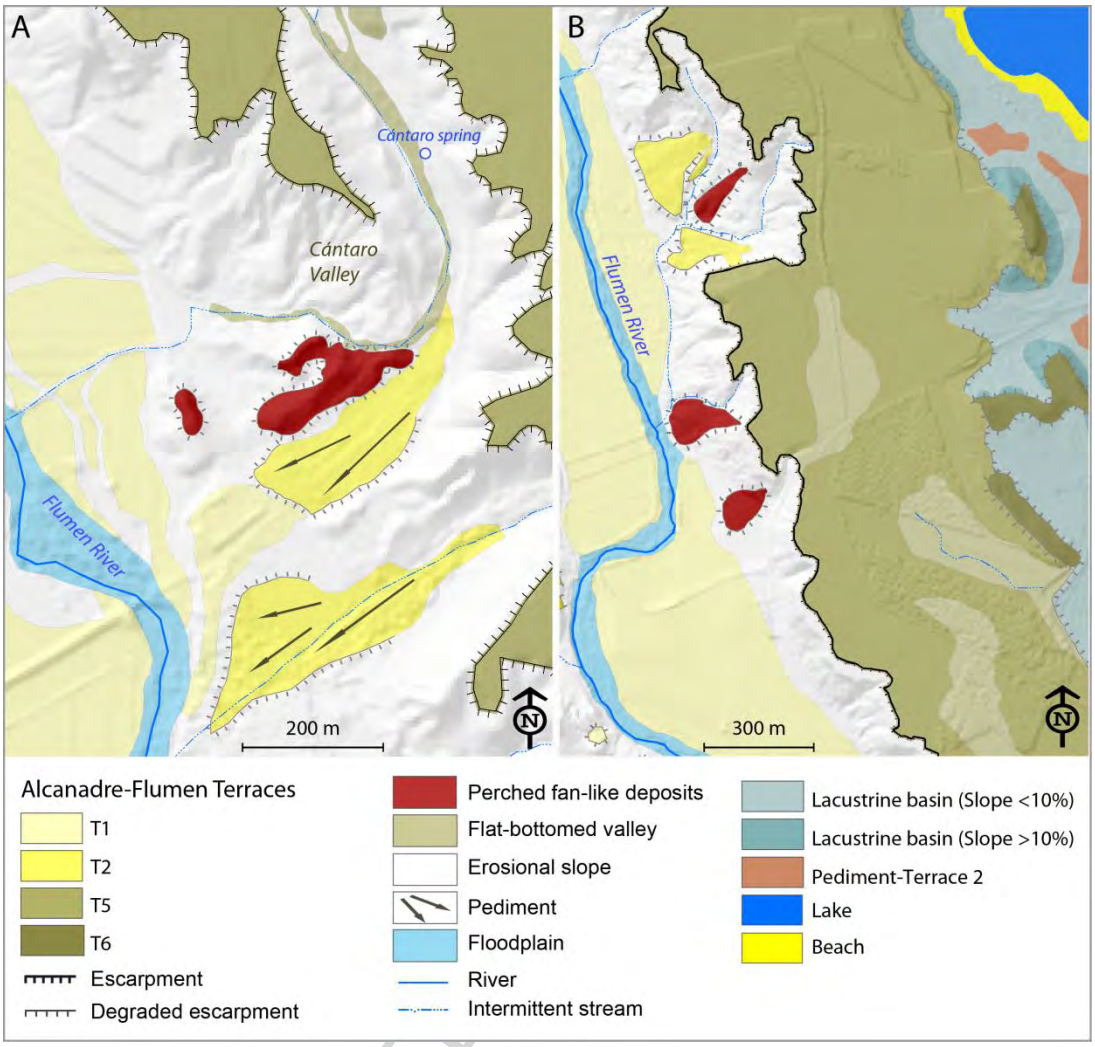

Fig. 11. Detailed geomorphological maps of the perched fan-like deposits of the western mesa slopes. The map is overlying the LiDAR-derived hill-shaded DEM. Location shown in Fig. 4.

Fig. 12. Longitudinal profile of a perched fan-like deposit at Cántaro Arroyo, mapped in Fig. 11A.

4.3. Geophysical profiles

The Laguneta profile, located to the south of the lacustrine basin, crosses the bottom of the flat-bottomed valley referred to in section 4.1 (Fig. 8). The resulting ERI model depicts two main resistivity layers: a shallow high-resistivity (> 500 Ωm), 1 to 3 m-thick layer interpreted to be the fluvial T5 deposit, and an underlying low-resistivity (< 150 Ωm) layer interpreted to be the Miocene clays with sandstones (Fig. 13A).

The seismic P-velocity model (Fig. 13B) shows three different seismic layers: a topmost low-velocity (300-500 m/s) layer, which may be the over-interpretation of the aerial wave together with the soil layer response; an intermediate layer with a velocity of ~1000 m/s, which broadly matches the fluvial deposit inferred in profile A; and a deeper, high-velocity (1500–2000 m/s) layer corresponding to the Miocene substratum.

The ERI profile shows how the contact between the fluvial T5 deposit and the Miocene bedrock is roughly irregular and discontinuous, especially on the SSW side of the profile, which corresponds to the valley bottom. Near the NNE edge of the profile, beyond the valley bottom, the contact is more planar and continuous, at about 3 m depth. The velocity model (Fig. 13B) shows a lower velocity gradient between the fluvial deposit and the bedrock within the valley bottom, indicating a less stiff bedrock and/or looser material than at the valley edge.

The ERI profile at the Puyalón site (Fig. 13C) represents the cross-section of a flat-bottomed, NNW-SSE oriented valley (Fig. 4). This profile, much deeper than that at Laguneta, also depicts a low-resistivity layer (< 50 Ωm) overlain by a high-resistivity layer (> 100 Ωm), interpreted as the Miocene bedrock and the overlying fluvial T5

deposit, respectively. Like the Laguneta profile, the contact between the two units (red dashed line in Fig. 13C), located at a depth of around 4–5 m, is quite irregular and discontinuous, especially below the valley bottom. A series of irregular, metric-sized voids, some more than 8 m wide and with a noticeable vertical elongation, can be identified within the Miocene substratum, at depths of 7 to 20 m below the fluvial T5 deposit. The red arrow in profile C indicates a very surficial signal about 6 m wide corresponding to the gravel infilling of a trench dug for the installation of the main NW-SE-oriented irrigation pipe. Other artefacts are ruled out at this shallow level where the high signal-to-noise ratio results in high sensitivity in the ERI model. The lower envelope of the major voids wedges out to the E while to the W it achieves a roughly horizontal geometry at about 30 m depth (white dotted line in Fig. 13C).

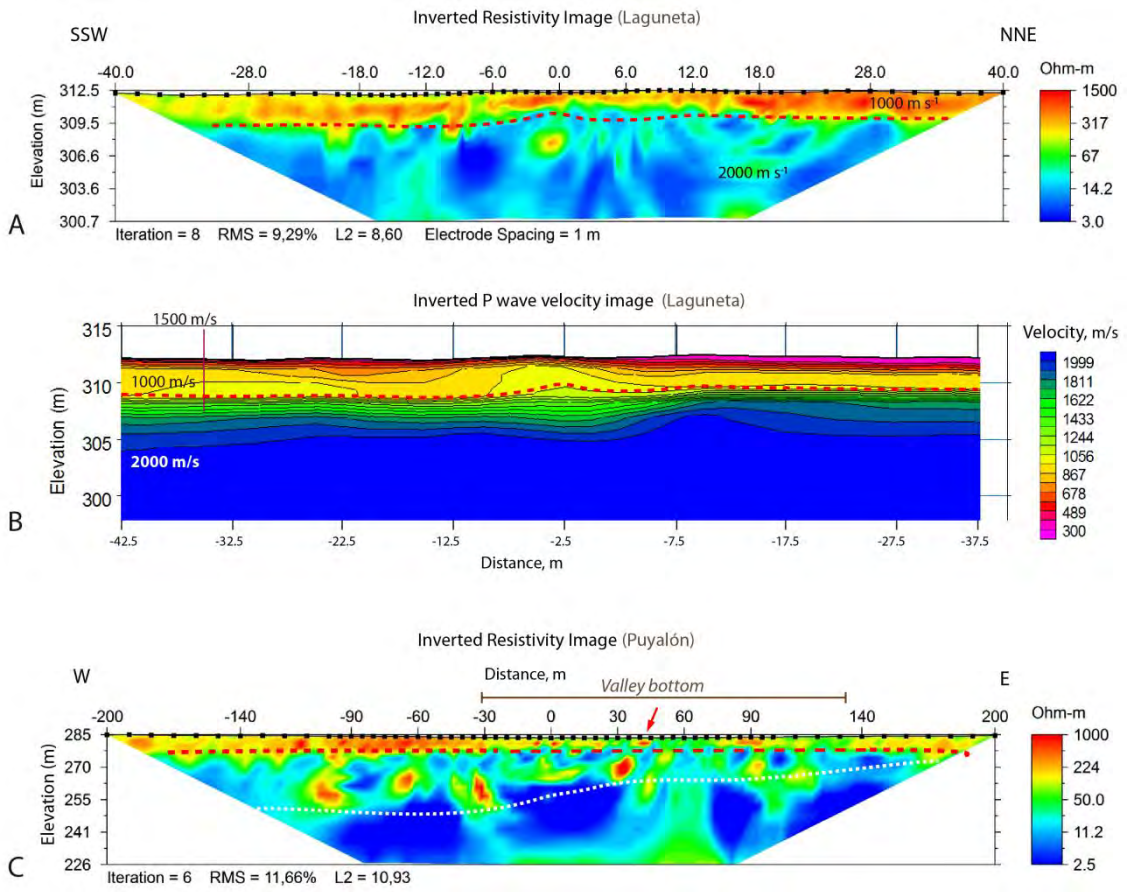

Fig. 13. Geophysical models of the subsoil architecture at the Laguneta (A and B) and Puyalón (C) sites. (A) Inverted resistivity image and (B) P-wave velocity model of the Laguneta profile. (C) Inverted resistivity image of the Puyalón profile. The red dashed lines define the base of the upper layer and the white dotted line in (C) represents the lower envelope of the major voids detected.

4.4. Soils and parent materials

Soils developed from the clayey Miocene materials are usually shallower than 2 m. Entisols and Inceptisols predominate in the geomorphological units of the Sariñena Basin (Fig. 7). Entisols are found on the highest slopes, where heterogeneous, shallow, and weak soil profiles develop. The less frequent Aridisols and Alfisols are associated with more ancient soils and exhibit clay mobilisation, coatings and natric characteristics. The most common Subgroups are Calcic Haploxerepts, followed by Typic Calcixerepts, Xeric Torriorthents, and Typic Xerorthents.

The Sariñena basin is characterised by the occurrence of soil salinity and sodicity in different topographic positions (Table 4), from the gentle slopes and upper terrace-pediment (PT3) down to the palustrine area. Btnk horizons incorporate materials affected by predominantly sodic salts (NaCl and Na_2SO_4). Their desalinisation favoured strong Na saturation of the cation exchange complexes in the soils and subsequent clay illuviation. The soil saturation extracts have a mean ECe = 6.0 dS m^{-1} (range = 1.5–29.7 dS m^{-1}) and a median sodium adsorption ratio (SAR) of 14.6 (range = 1.8–39.7). Many individual SAR values were much higher than the classical threshold of SAR for sodic soils (> 13). Following the salinity phases established for irrigated agricultural soils by the NRCS (Soil Survey Division Staff, 1993), moderately and slightly saline soils

predominate in the Sariñena basin. Exceptionally, very strongly saline soils are found in the PT2 pediment level (Fig. 7).

The soils have a mean calcium carbonate equivalent (CCE) of 25% and a very low organic matter content (mean = 1%). With the exception of the clayey soils in the palustrine area, the soils in the basin have a predominantly medium- to moderately-fine texture.

In the lower units, PT1 and the palustrine area, the common occurrence of redox features evidences inherited lacustrine conditions, i.e. soil saturation by water due to water-level fluctuations in the lake. The underlying Miocene materials, mainly fine detrital sediments, consist of mainly saline–sodic dispersible claystones with carbonates (mean CCE 22%) and predominant illites (≅ 75%). There is rare gypsum in the sandstones (Table 5).

Table 4. Selected soil data for pedons representative of the main geomorphic units in the Sariñena lacustrine basin (pHp: pH measured in the saturated soil paste; CEe: electrical conductivity of the saturated soil-paste extract; OM: organic matter; CCE: calcium carbonate equivalent; SAR: sodium absorption ratio).

Horizons*	Depth cm	pHp	CEe dS m^{-1} 25ºC	OM	CCE	Sand	Silt	Clay	USDA textural class	SAR
						%				
Pediment-Terrace 3/LN-1/Typic Natrixeralf										
Ap	0-22	8.3	8.08	0.82	17.0	30.6	31.3	38.1	Clay loam	16.8
Btn	22-40	8.3	3.72	0.85	17.0	37.9	29.3	32.8	Clay loam	11.2
Btnk	40-110	8.6	2.41	0.61	30.0	34.3	33.2	32.6	Clay loam	4.6
2C (lutite)	> 110	---	---		---	---		---	---	---
Pediment-Terrace 2/LO-21/Calcic Haploxerept										
A	0-23	8.2	2.19	1.48	24.0	19.7	27.6	52.6	Clay loam	3.6
Bwk	23-74	8.3	8.02	0.59	31.0	26.7	34.0	39.3	Loam	18.2
2Bwk	74-110	8.2	29.70	0.33	32.0	24.5	32.7	42.8	Loam	39.7
2CB	> 110	---	---		---	---		---	---	---
Pediment-Terrace 1/LO-7/Calcic Haploxerept										
Ap	0-27	8.7	2.05	1.34	22.2	49.5	28.3	22.2	Loam	5.3
Bwkg	27-93	9.1	2.17	0.57	25.5	52.9	21.6	25.5	Silt loam	6.9
2C (lutite)										
High slope (40%)/LO-3/Xeric Torriorthent										
A	0-32	8.2	2.23	2.87	30.0	21.3	43.2	35. 5	Loam	4.4
2C (lutite)	32-53	---	---		---	---		---	---	---
Low slope (5%)/LO-6/Typic Xerorthent										
A1	0-20	8.5	1.49	0.92	30.0	21.	42.9	36.1	Loam	3.3
A2	20-40	8.7	5.46	0.66	33.0	25.4	50.2	24.4	Silt loam	14.4
Bwy	40-68	8.2	2.97	0.17	6.0	26.6	69.6	3.8	Silt loam	1.8
2Cy (lutite)	68-80	---	---		---	---		---	---	---
Palustrine depression/FL-2/Sodic Calcixerept										
Ag	0-18	7.9	4.66	1.27	23.4	45.7	39.2	15.1	Clay	14.9
Bwg1	18-35	8.3	5.39	2.47	16.9	55.4	38.1	6.5	Clay	19.6
Bwg2	35-60	8.6	5.62	0.91	12.3	54.4	34.8	10.8	Clay	21.3
Bwkg1	60-95	8.7	6.73	0.71	24.1	59.1	33.0	8.0	Clay	22.8
Bwkg2	95-120	8.5	7.91	0.63	33.0	53.0	35.2	11.8	Clay	25.4
2C	120-160	8.5	7.91	0.52	30.5	45.9	32.5	11.8	Clay	25.4

* The meaning of the lowercase letters used as suffixes to designate specific features within the soil master horizons (A, B, and C) are as follows: g, strong gleying; k, accumulation of secondary carbonates; n, accumulation of sodium; p, tillage; t, accumulation of silicate clay; w, development of colour or structure; and y, accumulation of gypsum (Soil Survey Staff, 2014).

Table 5. Selected characteristics of the claystones and sandstones in the Sariñena lacustrine basin (Locations shown in Fig. 7). CCE: calcium carbonate equivalent; Gyp: gypsum; pHp: pH measured in the saturated soil paste; CEe: electrical conductivity of the saturated soil-paste extract; SAR: sodium absorption ratio.

Sample	Sand	Silt	Clay	CCE	Gyp	pHp	CEe	SAR	Clay minerals of oriented aggregates, %		
	%						dS m^{-1} 25 ºC		Quartz	Calcite	Illite
Lutites											
L1 (LAG-1)	2.2	58.1	39.7	18.6	0	8.5	12.9	29.5	4	17	76
L2 (LAG-2)	4.1	52.0	43.9	24.1	0	9.1	8.1	33.3			
L3 (AG-4)	3.9	47.6	48.5	24.7	0	8.6	18.6	49.2			
L4 (CP-21)	5.9	53.2	40.8	12.3	0	8.3	12.2	29.4	8	13	71
Sandstones											
A1 (AR-1a)	70.9	21.0	8.1	28.2	0						
A2 (AR-1b)	54.4	39.0	6.7	32.8	0						
A3 (AR-2a)	88.8	7.2	4.1	16.8	0						
A4 (AR-2b)	79.9	12.2	8.0	15.5	14.3						

5. Discussion

Most lacustrine depressions in the central Ebro Basin hold playas and saline lakes, whose geomorphic origin and evolution remains poorly understood (Gutiérrez et al., 2013). Lake genesis models applied to the region include the collapse of large bedrock cavities, widespread dissolution by groundwater and subsequent subsidence, and aeolian deflation during dry periods (Quirantes, 1965; Ibáñez, 1975; Sánchez et al., 1998; Gutiérrez et al., 2013). Sariñena Lake, one of the most important bodies of water in the Ebro Basin because of its size and volume, is difficult to explain using these models. Its

morphology and dimensions, the nature of its substratum and the absence of related aeolian deposits rule out the genetic models proposed by other authors (Ibáñez et al., 1984; Hernández Samaniego et al., 1998). The results of this work show how the formation and development of this lake are the consequence of various factors and processes, among which piping plays a significant, although not exclusive role. The following discussion focuses on reconstructing the initial conditions under which the proto-lacustrine depression was generated, and then goes on to address the processes involved in the development of the basin until it reached its present-day form.

5.1 Origin of the lacustrine depression

The genesis of the Sariñena high plain is interpreted in the context of the evolution of the main fluvial network draining the southern Pyrenean ranges. There was very active lateral migration of channels as well as river capture processes along the Pyrenean piedmont during the Pleistocene. Wide alluvial mantles formed on the southern Pyrenean piedmont, favoured by the easily eroded materials and topographic lows between the mountain ranges and the limestones of the central Ebro Basin (Fig. 2). The formation of extensive terrace levels, many of them acquiring a fan-like shape in plan view, could have been related to allogeneic factors such as climate change and uplift episodes in the Pyrenean ranges, as well as to avulsion processes during their evolution (Alberto et al., 1984; Rodríguez-Vidal, 1986).

The Sariñena T5 high plain is an example of the rapid lateral migration of the Alcanadre River during the middle Pleistocene. According to Calle et al. (2013), the sedimentological characteristics of the Alcanadre River terrace deposits suggest that the higher levels represent braided channels with a very strong tendency for lateral migration, while the lower terraces are associated with increasing channel confinement

and river incision. The T5 terrace level of the Sariñena plain is a clear example of these braided channels, not only because of its remarkable lateral extension but also the sedimentological characteristics of its main unit (lower unit in Fig. 6). The lateral migration of the Alcanadre River was restricted on its eastern side by an important topographic barrier represented by various levels of high terraces (Fig. 4), which forced the prevalent lateral migration of the river towards the W. This westward migration was in turn constrained by the remnants of a series of higher, earlier terraces that formed the interfluvial area between the Flumen and Alcanadre rivers (Fig. 14A).

The high mobility of the Alcanadre channel generated a fan-like alluvial plain that corresponds to the northern half of the Sariñena high plain, north of the present lake (Figs. 4 inset and 14B). High flood stages during the development of the T5 alluvial plain would have caused the generation of overbank and crevasse-splay sheets, typical of highly fluctuating rivers, especially in semiarid environments (Bridge and Demicco, 2008; Li and Bristow, 2015). The topographical restrictions on the eastern valley side favoured the development of widespread overbank deposits on the western margin of the valley (Fig. 14B). This produced a fluvial fan-like deposit, which can be interpreted as a large crevasse splay. This deposit is recognisable in the centre of the high plain, overlying preceding channel facies (Fig. 6). The finer grain size of the deposits and the low-angle cross stratification is typical of this kind of facies (Pontén and Plink-Björklund, 2007; Van Toorenenburg et al., 2016), and its lateral continuity is indicative of rapid progradation. The exposed section shown in Fig. 6 suggests there was more than 6 km of westwards progradation (the current width of the Sariñena mesa), although the present-day geometry of the mesa (Fig. 4 inset) indicates progradation was more likely towards the SW (Fig. 14C). Crevasse sheets typically develop a basal erosion surface (like that recognisable in Fig. 6) and a metre-scale thickness that decreases

towards the distal margin, thinning gradually or ending abruptly with a steep slope (Bridge, 2003). In this sense, the topographic profiles in Fig. 5 resemble those described in many other mature fluvial systems with well-developed floodplains and crevasses (Coleman, 1969; Smith et al., 1989; Mjos et al., 1993). At present, there is a height difference of 2-3 metres between the E (proximal) and W (distal) T5 margins.

Subsequently, a typical backswamp area is expected to have formed in the distal areas of the crevasse lobes, overlying the fine sediments deposited previously on the floodplain, as observed in the T5 deposits (see Section 4.1). It is likely that this swamp, or palustrine area, hosted intermittent standing water between the high terrace footwall and the crevasse sediments (Fig. 14C). At a later stage, the lateral migration of the Flumen River and its tributaries towards the E would have partially eroded the remnants of the higher terraces. After this, the incision of the Alcanadre River would have led to the generation of an incipient fluvial network on the T5 level, forming smooth flat-bottomed valleys on the high plain. The existing palustrine area became perched and was preserved probably due to its significant extent and remarkable isolation with regard to distance to the Alcanadre River valley. From an evolutionary point of view, this can be considered the starting point in the genesis of the Sariñena depression. It is highly likely that in this embryonic stage the depression would have been characterised by very gentle slopes and intermittent, shallow water (Fig. 14D).

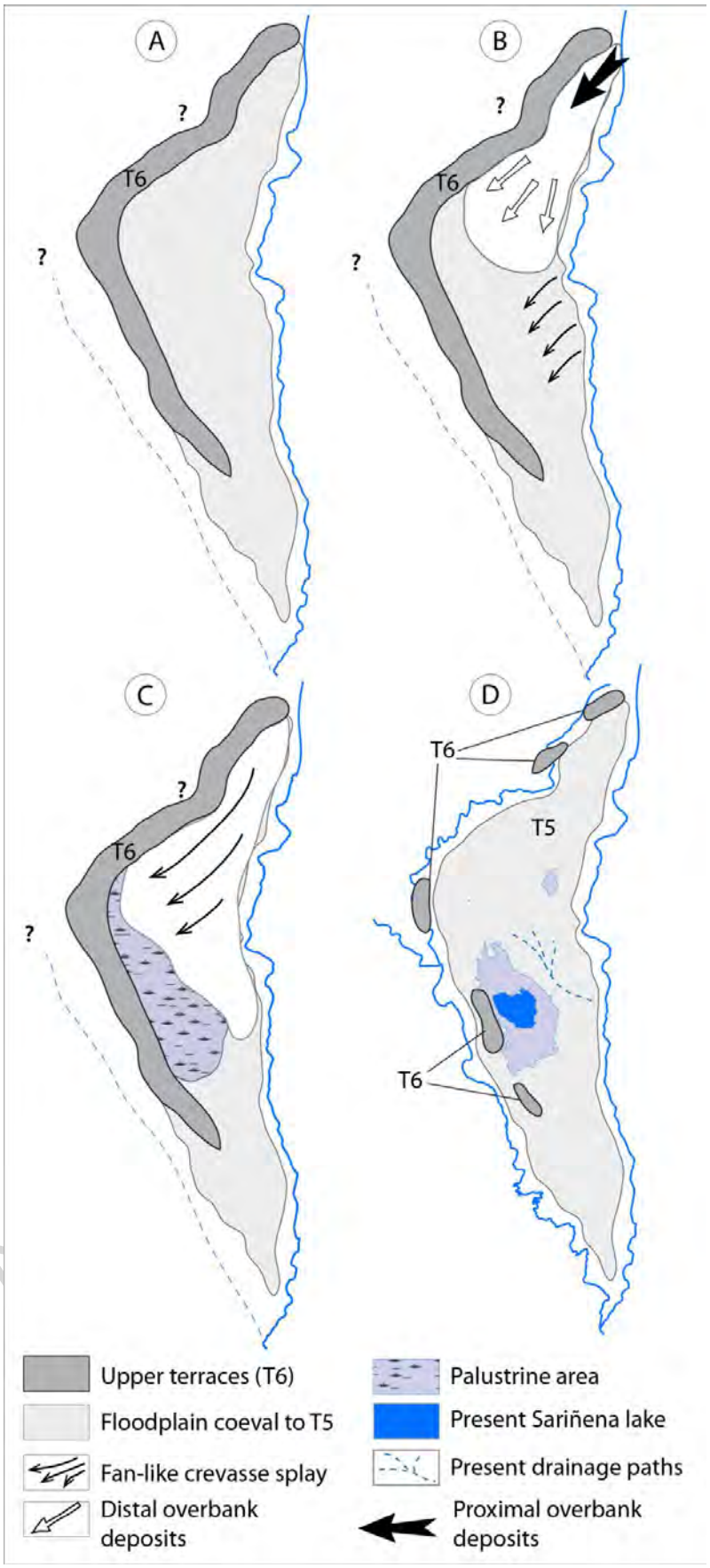

Fig. 14. Simplified sequence illustrating the formation of the Sariñena depression.

5.2. The role of piping processes in the evolution of the basin

Climate, geomorphology, topography and substrate characteristics provide clues for reconstructing the evolution of the Sariñena Basin related to piping processes. Traditionally, the development of piping has been associated with the presence of several conditioning factors: climate, physiography, and the inherent properties of soils or sediments (Jones, 1981; Bryan and Yair, 1982; Selby, 1982; Parker et al., 1990; Jones, 1994, 2004; Faulkner et al., 2000, Desir and Marin, 2011; Goudie, 2013). Piping only occurs in soils with a high dispersion index, sodium content, SAR and exchangeable sodium percentage. Nevertheless, these factors alone do not automatically lead to piping, as this process also requires seasonally variable rainfall, a high soil cracking density, suitable slope length and gradient, together with a high hydraulic gradient, scarce vegetation cover, and relatively impermeable layers in the soil profile promoting an irregular horizontal subsurface flow.

In the central Ebro Basin, soil loss by piping is especially amplified in unconsolidated materials (mainly silts and clays) due to irrigation and the saline nature of the soil (García-Ruiz et al., 1997; García-Ruiz, 2011; Gutiérrez et al., 1997). In the Sariñena Basin, the salinity and sodicity of the soils and Miocene sediments, together with the low organic matter content of the soils (Tables 4 and 5), promote the structural instability and dispersibility of materials and their transport through the subsurface, as well as conspicuous surface soil erosion. Soil salinisation and sodification processes, and elevated SAR values were identified decades ago in the Flumen area (Lebrón, 1988; Rodríguez-Ochoa et al., 1990, 1999; Vizcayno et al., 1995; García-González et al., 1996; and Sirvent et al., 1997), related to lithological, geomorphological, climatic and anthropic factors. Oedometric assays carried out on these Miocene clays gave swelling

values of up to 12% (Gutiérrez et al., 1997). The occurrence of sand and clay coatings in the pipes (Pratdesaba, 1997) confirms the high transport capacity of the flow. Soil loss, pipe erosion, water logging, pipe-drain clogging, and land abandonment have been recurrent problems in the area (Herrero et al., 1989; Rodríguez-Ochoa et al., 2000; Darmendrail et al., 2004). Evidence for this can be observed in agricultural areas subjected to intense levelling without preservation of the topsoil and after the modernisation of irrigation (Rodríguez-Ochoa et al., 1989; Rodríguez-Ochoa and Artieda, 1999). Outstanding evidence of active piping processes has been described in the basin (see Section 4.2, Figs. 9C and D), as well as in nearby areas (Figs. 15A and B; Harvey and Gutiérrez-Elorza, 2005; Gutiérrez et al., 2002b).

Similar conditions favouring piping are supposed to have taken place in the Sariñena basin during its evolution. In fact, there is direct and indirect evidence of relict piping processes in the zone. The palaeocollapse shown in Fig. 10 is an example of an ancient subsidence episode affecting the T5 fluvial deposit. The perched fan-like deposits identified in the western slopes of the T5 high plain (Figs. 11 and 12) indicate past piping activity. According to their geometry, topographic position and composition, these deposits are interpreted to be outlet deposits related to the subsurface transport and evacuation of gravel-rich materials from the high terrace levels. Only the Cántaro fan (Figs. 11A and 12), located in the middle of a valley, may involve a certain surface component linked to supply from the Cántaro River. Quite similar gravel-rich, fan-like outlet deposits were reported by Batalla and Balasch (2001) as a consequence of piping processes affecting an earth dam in Altorricón (central-eastern Ebro Basin), which eventually led to the catastrophic failure of the structure. The genetic interpretation of the fan-like outlet deposits is supported by the abundance of subsurface voids recognised in the Puyalón geophysical profile, the location of which was selected

according to two main geomorphic indicators: 1) the active landslides on the steep slopes of the southwestern and southern margins of the Sariñena Basin (Fig. 7) indicative of recent and/or present subsidence processes; and 2) the proximity to the hypothetical main line of subsurface flow and particle transport between the lake basin and the nearby outlet deposits. The voids in the Puyalón profile probably represent a dense network of conduits developed at the lower contact between the fluvial deposit and the Miocene substratum (Fig. 13A), as well as within the Miocene clays (Fig. 13C). The remarkable size of the voids (8–12 m) and their depth (7–20 m) indicate important subsurface erosion due to piping. There are examples of similar, or even larger voids in the nearby Clamor Valley (Figs. 2, 9C and D) developed in Holocene valley fills fed from the erosion of the same Miocene units as in the Sariñena area (Harvey and Gutiérrez-Elorza, 2005) (see Fig. 13.24, page 307 in Gutiérrez-Elorza, 2005). Besides the size and depth of the voids, the irregularities in the ERI profiles at the base of the fluvial deposit reveal that the complexity and degree of development of the subsurface pipe network increase towards the W, where the Flumen River valley represents the local base level of the hydraulic gradient responsible for piping initiation and enlargement.

Usually, piping outlets are open conduits through which water and/or sediments have been evacuated (Jones, 1981, Goudie, 2013; Harvey, 1982; Romero-Díaz et al., 2007) but there are limited records and evidence of outlet deposits, even where rock blocks have been removed through the conduits (Parker et al., 1990), similar to karst environments (see Fig. 1 in Rodríguez et al., 2014). The piped materials are generally silts and clays, which are easily eroded once released from the pipe system. However, gravel deposits can also be involved in piping, even if this initiates in finer, more susceptible horizons, as reported by Ternam et al. (1998). A spectacular example of pipe

growth involving the base of a capping gravel deposit can be seen at Bardenas Reales Natural Park, in the western Ebro Basin (Fig. 15C).

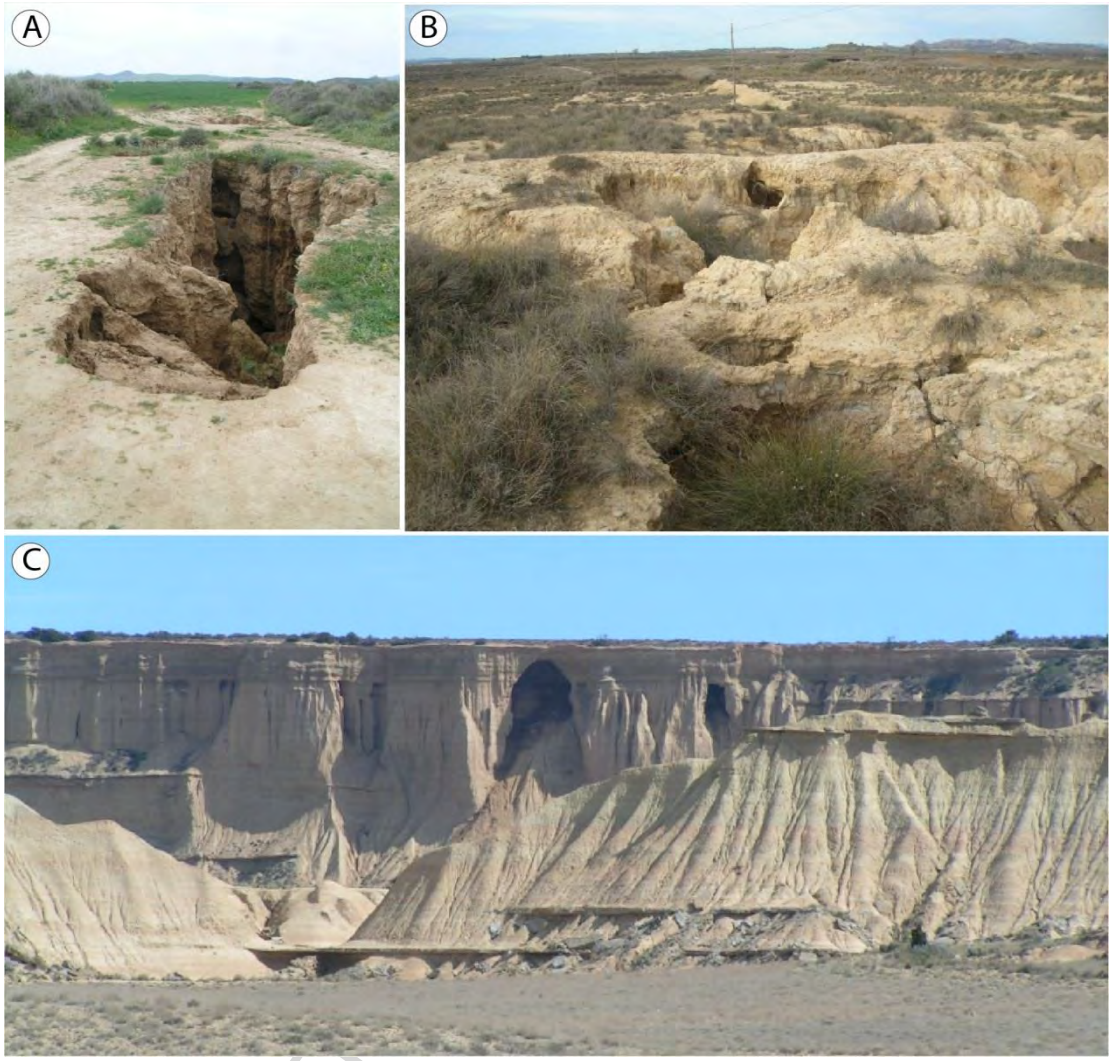

Fig. 15. Examples of piping processes in the Ebro Basin. A and B) Initiation and development of piping-related depressions on horizontal surfaces near the Sariñena Basin. C) Gravel cap undermined by pipe growth in Miocene clays, Bardenas Reales Natural Park.

Similarly, the pipes in the Sariñena Basin originated in the Miocene bedrock due to water infiltrating across the interstitial porosity of the capping fluvial gravels into the Miocene clays. Voids and conduits very likely formed initially in the contact between the two materials and progressively grew horizontally until finding an exit or outlet

depending on the prevailing hydrological gradient: to the west in the case of the Sariñena Basin, or to the east for Laguneta Lake. Once the outlet was established, subsurface flow circulation promoted enlargement of the pipe through which eroded material was evacuated. The pipe network progressively reached a higher hierarchical organisation, favouring the increased drag and transport capacity of the water flow. This piping enlargement would have been especially rapid during phases of Alcanadre and Flumen river incision, due to the concomitant increase in the hydraulic gradient.

Pipe enlargement involved removal of the base of the capping T5 fluvial deposit. Erosional emptying of pipes and the loss of caprock cohesion finally led to collapse. Coarse detrital material, including gravels, was transported through the voids, as suggested by the irregular contact at the base of the fluvial deposit (Fig. 13). Very likely some of the voids were filled by gravels (Fig. 13C). All this evidence points to piping as the main cause of subsidence and recent morphological development in the Sariñena Basin.

In a similar way, the Laguneta lacustrine basin (Fig. 8) can be considered to be a small collapse, evidenced by the subvertical escarpments bounding the S and SE basin margins and the presence of a perched flat-bottomed valley starting in these margins and oriented towards the Alcanadre Valley. The floor of this flat-bottomed valley and its NE margin were selected for geophysical surveying. The very irregular contact between the fluvial deposit and the Miocene substratum in the centre of the valley (SW side of the ERI profile, Fig. 13A) reveals significant development of piping conduits below the valley floor, suggesting that the origin of the valley and its perched location may be linked to piping–related subsidence with subsurface drainage towards the SE (Fig. 8). The possible outlets would be located more than 1 km from the lake and are not visible due to the intense transformation of the area by linear infrastructures (railway and

roads) and agriculture. The magnitude of piping development and associated subsidence in Laguneta is much more limited than in Sariñena Lake, and is related to water draining towards the E slope of the Sariñena high plain. In this case at least two episodes of land subsidence linked to piping can be inferred. The first would have been responsible for the generation of the flat bottom valley, reflecting the prevailing subsurface flow from the centre of the T5 plain towards the Alcanadre River valley. The second, subsequent episode generated the Laguneta depression, inset into the T5 plain, leaving the flat-bottomed valley perched with respect to the base of the depression.

5.3. Evolution of the Sariñena Basin

The hypothesis proposed for the evolution of the Sariñena Basin requires the following steps:

1) Blocking relief (T6 terrace levels) created confined areas that occluded a low-lying zone where water was available and there was no external surface drainage (Fig. 16A).

2) A significant hydraulic gradient was generated that was high enough for piping processes to develop in the Na-rich Miocene clays. Pre-existing structures such as joints and palaeochannels in the sandstones would have favoured preferential flow pathways underneath the T5 terrace, as noted by Higgins and Schoner (1997). This gradient became progressively higher during the vertical incision of the Alcanadre and Flumen rivers during the Middle and Upper Pleistocene, according to dating by Calle et al. (2013). The dimensions of the initial pipes probably ranged from cm to dm, similar to those described by Khobzy (1972) in the genesis of closed depressions in areas of smooth relief (Figs. 15A and B). Excavation by piping was favoured by the alternation of humid and dry periods (Fig. 16B), since water table oscillations induce changes in the hydraulic gradient. During dry periods with higher gradients, vertical growth of

pipes would have prevailed thanks to the circulation of undersaturated hypodermic fluxes, while in humid periods, when the water table was higher, there would have been horizontal development of the pipe network and conduit enlargement.

3) Pipes and conduits became large enough to allow the transport of gravels from the capping terrace deposit, and the basin floor subsided due to successive collapses. Since the water level in the lake was probably related to the regional water table, these pulses would have led to the intermittent desiccation of Sariñena Lake and the exposure of the former lake floor to surface water erosion processes. After each river incision episode, the topographical gradient produced between the desiccated lake floor and the new surrounding river floodplains would once again have favoured the onset of piping processes along the Sariñena floor. These processes would have generated erosional micro- and macroforms typical of low-gradient surfaces submitted to piping, similar to those that can be observed at present in the area (hollows, pseudo-dolines and collapses, natural bridges, etc.; Fig. 15A), with a roughly irregular bottom surface being produced over time (Fig. 15B).

The increasing verticality of the surrounding slopes triggered the development of mass movements and erosion by water. As a result, the slopes retreated and the basin widened evolving a U-shaped cross-section (Fig. 16C). Intervening phases of stability would have favoured the development of the PT levels, coeval with the deepening and flattening of the depression bottom. The presence of small escarpments separating the different pediment levels indicates that at least three basin-bottom deepening phases took place during the evolution of the depression, probably related to successive lowering of the hydraulic gradient and the rejuvenation of the piping system, separated by phases of stable water levels. The base levels of the Sariñena pediment-terraces are broadly equivalent in elevation to those of the Alcanadre-Flumen T4 and T3 terrace

levels (Table 3), suggesting that the systems were genetically connected through oscillations in the water table, as a response to the regionally alternating episodes of river incision and alluviation.

Regarding the period of development of the lake, the only data which can be referred to is the relationship of the lake height to the different Alcanadre River terrace levels and their respective dates supplied by Calle et al. (2013) and showed in Table 2. According to this, T5 level may have an estimated age equal to or younger than 780 ky BP. The bottom of present Sariñena Lake develops at a height equivalent to T3 level, with an estimated age between 44 and 19 ky BP. Finally, the fan-like deposits developed in the eastern flank of the Flumen River valley are coeval with the T2 terrace level of the Flumen River system, whose age can be estimated about 19-10 ky BP. The age of such outlets probably corresponds to the main and last period of collapse in the Sariñena depression, coeval to the development of T3-T2. In summary, very likely the main episodes of Sariñena Basin development occurred during the Last Glacial Maximum. Palaeoclimatic studies of lacustrine records in nearby lakes of the Ebro Depression during that period indicate the prevalence of semiarid cold steppe vegetation with an increase of the effective moisture which made some lakes to experience more positive water balance than today (Valero-Garcés et al., 2004).

During humid periods, water would have accumulated more frequently in the basin, enabling wind-generated waves to flatten and level the lake bottom, a planation process common in shallow lakes (Lees and Cook, 1991). This basal erosion of the lake by waves would have led to the entrainment and transport of debris over the rough, irregular floor left after the previous period of desiccation and piping activity. Finally, eroded material would have been exported through the dense conduit network excavated in the lake substratum, towards the surrounding river valleys. As reported by Batalla

and Balasch (2001), active pipes can evacuate material very quickly, producing a very high sediment yield, such as would have been required to excavate the significant volume of Sariñena basin (estimated to be approximately 30×10^6 m^3). The presence of numerous outflow pipes in the erosive slopes surrounding the Sariñena high plain reinforces this hypothesis.

4) Some conduits and voids became filled and obstructed by gravels (Fig. 13C), and very probably became inactive. In other cases, the smaller grain size of the gravels or the greater dimensions of the pipes allowed subsurface gravel transport until this finally exited into the Flumen River valley, and formed the fan-like outlet deposits, coeval with the T2 terrace of the Flumen River valley (Fig. 16D).

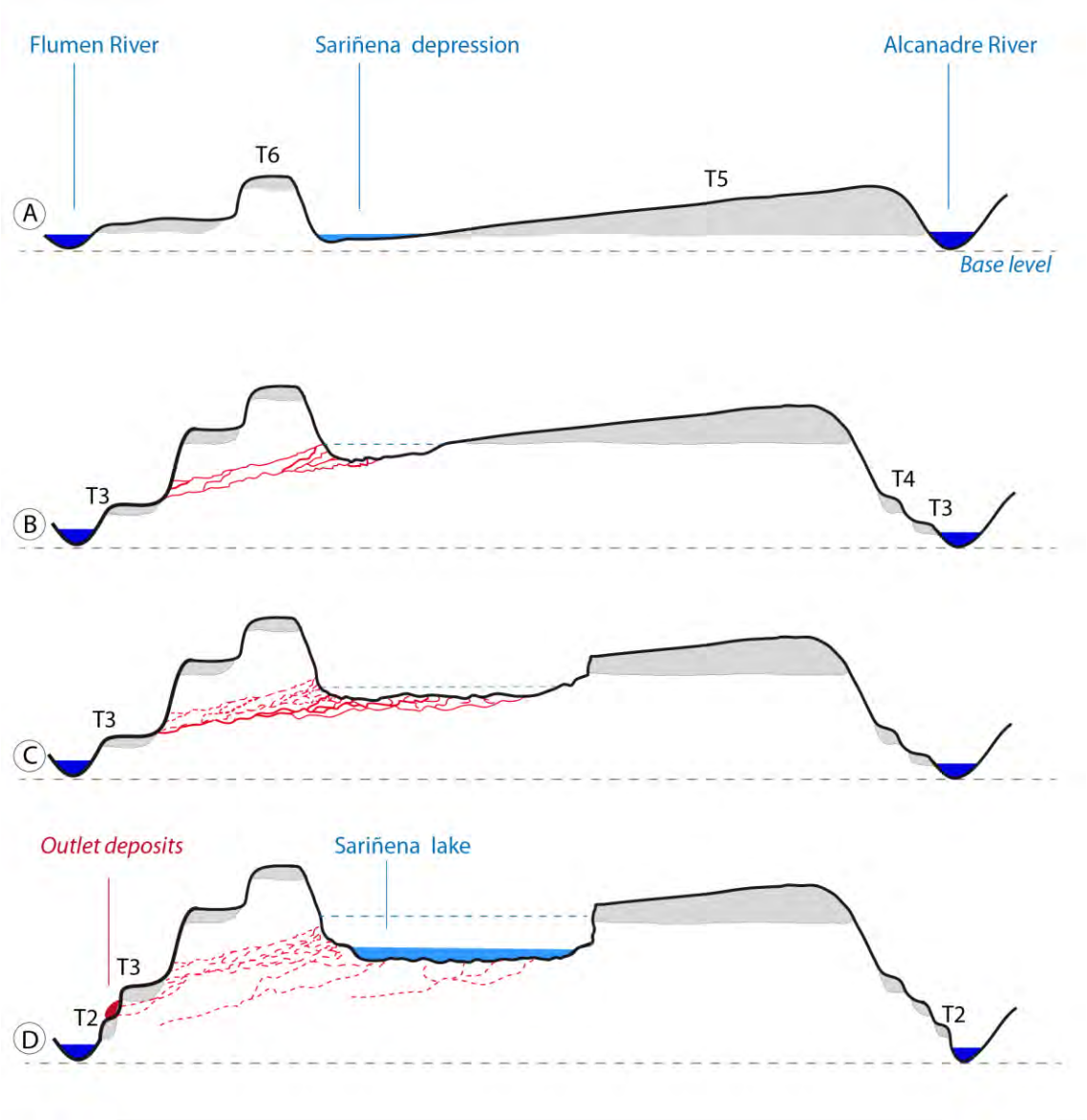

Fig. 16. Conceptual model for the genesis and evolution of Sariñena Lake.

The prevailing NW winds produce small waves (ranging between 0.2 and 0.3 m) on the lake surface and some coastal dynamics consisting of minor littoral spits and sand barriers that reflect a prevailing clockwise shoreline current. It is likely that this current is responsible for redistributing the sediments around the lake shores, preventing the accumulation of deposits on the lee side (Fig. 7). The action of wind-produced waves must have always occurred under conditions of reduced water depth, meaning active interaction between the waves and the lake floor, a very frequent feature of shallow

lakes in semiarid environments (Lees and Cook, 1991). The resulting lake bottom sediments eroded by the waves are subsequently transported and distributed along the lake bottom.

At present, many minor pipes can be recognised in the basin floor. Sariñena Lake water is supplied by the current irrigation surplus and has low salinity and sodicity. These undersaturated waters may circulate as hypodermic fluxes until they reach the present water table, favouring the initiation of piping. Several springs rise in intermediate and low topographic positions on the western slopes of T5, facing the Flumen River valley (visible in the aerial photographs from 1927 and 1957). Sudden pipe collapses could occur in the future, mobilising and exporting clay, although their dimensions would probably not be large enough to generate sufficient flooding to transport gravels. The future of the system may involve the rejuvenation of piping erosion once the base level drops due to fluvial incision (Fig. 16D) and the hydraulic gradient increases because of the migration of the Flumen River towards the E.

5.3. Piping-derived lakes: a new type of lake origin?

There are very few examples in the literature of lakes and closed depressions generated by piping. Wright (1964) interpreted piping to be the main formational factor in the genesis of hundreds of lakes developed on siliceous sands and sandstones in the Chuska Mountains, northwestern New Mexico. In this case, successive episodes of water table lowering were inferred to have occurred during the Pleistocene producing the depressions, which at present are considered relict forms. Khobzi (1972) described pseudokarstic depressions in some parts of the Andes in Colombia, developed on siliceous alluvium and sands derived from the weathering of siliceous rocks. According to this author, piping can be directly observed in some cases and seems to be the initial

and perhaps the main lake-generating process. Higgins and Schoner (1997) explained the development of sinks on flat or nearly flat drylands, referring to a lowered water table and deep dewatering of the sediment. The onset of a strong inflow enlarges conduits and cracks, leading to the generation of sinkholes, even in gravel bodies. Huddart and Bennett (2000) described subsidence processes in an Icelandic proglacial lake bed caused by sediment cracking and subsequent subsurface piping. Shaw and Bryant (2011) also indicated piping as a mechanism that may be locally important in the generation of shallow lakes and pans in semiarid environment.

Although relatively rare, piping-related lakes and depressions constitute a particular type of basin that may appear in a wide range of climatic or geomorphic contexts, always associated with specific favourable factors, such as dispersive soils and hydrological gradients. However, no mention is made of this kind of lake in classical genetic lake taxonomy (Hutchinson, 1957; Reeves, 1968; Bayly and Williams, 1973; Timms, 1992). The latter two proposals are probably the most complete and detailed, and both differentiate between lakes related to processes like tectonism, volcanism, landslides, glaciation, solution, fluviatile action, wind action, coastline dynamics, biological activity, meteorite impact, and human action.

In some aspects, the origin of piping-generated lakes could be considered similar to that of lakes developed on confined floodplains, especially the fluviatile dams described by Timms (1992, pp 105), i.e. generated in blocked conditions associated with alluvial fans and laterally confined lowlands. However, Sariñena Lake does not correspond to the typical lake formed at the abrupt termination of the distal margin of the crevasse splay deposit (Bridge, 2003), although its early origin could have been associated with this kind of morphosedimentary setting.

As a premise, Sariñena Lake could be considered to have had a destructive origin, according to the early classification proposed by Davis (1882) for continental semiarid regions. Destructive forms generated by piping have been termed pseudokarstic. In fact, the term "pseudokarst" (Quinlan, 1966) has been often used for describing sinkholes and caves similar to those formed by karst although generated by processes other than the dissolution of substrata. The proper use of such a controversial term was discussed by both Otvos (1976) and Eberhard and Sharples (2013). Typical pseudokarstic forms generated by piping processes include caves and sinkholes, usually of limited size (Bartolomé et al., 2015).

Piping processes can be active in a number of geomorphic contexts and, as in the case of karst, depend on the existence of favourable substrata and hydraulic gradients. In several genetic aspects piping-related lakes and karstic lakes bear similarities to each other, since both are related to the removal of subsurface materials and can produce either gentle depressions or deep sinkholes. In this sense, one possible option would be to consider a class of "lakes generated through the removal of subsurface substrata", which includes both genetic types. In fact, the genesis and development of subsurface voids and conduits constitute the response of a specific substratum (regardless of whether this involves carbonate or Na-rich clays) to physical and chemical processes driven by flowing water under a given hydraulic gradient.

6. Conclusions

Sariñena Lake is a controversial wetland to which previous, traditional hypotheses on the origin of many lakes in the Ebro Depression cannot be applied. It could be considered to have had a destructive origin, in a semiarid continental context, where solution processes and wind action can be ruled out. The present morphology of the

lacustrine basin, characterised by high topographic gradients and steep slopes, the nature of the Miocene substrata underlying the lake, formed of insoluble dispersive clays and silts, and the virtual absence of aeolian forms and deposits, preclude a possible karstic or hydro-aeolian origin. The climate, bedrock and soil all favour pipe development, not only on the Sariñena high plain but also across a relatively wide area in the southern Pyrenean piedmont at the centre of the Ebro Basin. Piping micro- and mesoforms are quite common in the lake basin and surrounding areas, often being spectacularly developed and reaching impressive dimensions. Surface evidence of past collapse episodes affecting the main Pleistocene fluvial unit into which the lake is inset supports an initial piping-related genetic hypothesis. Detailed geomorphological mapping and field work was complemented with mineralogical and geochemical analysis of the soils and rocks, as well as a high-resolution geophysical survey. The results obtained evidence how piping processes are the main agent responsible for the basin evolving into its current form.

The onset of favourable conditions for the initiation of piping in this specific zone is not known in detail, although sedimentological data from the Pleistocene fluvial deposit on which the lake formed provides some valuable clues. The upper depositional level identified, and interpreted as a very wide crevasse splay, could explain the origin of the initial depression, as a backswamp area inset between the crevasse splay deposits and other confining relief. Subsequent evolution of the initial wetland would have been controlled by water table oscillations within a general falling trend, related to the incision/alluviation episodes recorded in the surrounding fluvial valleys. Episodes of fluvial incision favoured a prevailing vertical development of pipes, while episodes of alluviation and water table stabilisation promoted the enlargement and predominantly horizontal development of the pipe network. The general evolution of the pipes included

an initial phase in which a complex conduit network was constructed, and a further phase involving the lengthening of the pipes until they reached the base of the Pleistocene fluvial deposits. After this, some of the fluvial gravels were transported and exported to the nearby fluvial valleys through the subsurface pipe network, while other clasts filled up and blocked a number of pipes, halting their activity. At present only minor piping processes are still active on the lacustrine basin bottom and slopes.

A number of other minor closed depressions excavated in Miocene dispersive clays can also be recognised in the Ebro Basin, the origin of which is difficult to explain using traditional models. Undoubtedly, further research is necessary, particularly in light of the new evidence presented in this work. The results obtained from Sariñena Lake may aid in the reinterpretation of other controversial or poorly-understood closed depressions and lakes. Future research in this field will help support and reinforce the proposal of piping-related lakes, or lakes generated through the removal of sub-surface strata, if karstic lakes are also included, as a new genetic type of lake.

Acknowledgments

This work has been supported by the Ministry of Economy, Industry and Competitiveness under the project BASIL [PCIN-2014-106] and by the Spanish Research Council (CSIC) under the project Icoop-2016SU0015. We acknowledge the data provided by the Spanish Meteorological Agency (AEMET) after contract no L2 990130734. LIDAR data were supplied by the National Geographic Institute of Spain (Instituto Geográfico Nacional). Two anonymous reviewers have helped to improve the paper.

References

Alberto, F., Gutiérrez-Elorza, M., Ibáñez, M.J., Machín, J., Peña Monné, J.L., Pocoví, A., Rodríguez Vidal, J., 1984. El Cuaternario de la Depresión del Ebro en la región aragonesa. Cartografía y síntesis de los conocimientos existentes. Universidad de Zaragoza y Estación Experimental de Aula Dei, Zaragoza, 217 pp. Available at http://hdl.handle.net/10261/129421, accessed on 20-02-2017.

APHA, 1989. Standard Methods for the Examination of Water and Wastewater. 17th ed. American Public Health Association, Washington D.C. 1, 268 pp.

Aramburu, P., 1904. Las saladas de Sástago. Boletín de la Real Sociedad Española de Historia Natural 4, 428–429.

Arenas, C., Pardo, G., 1999. Latest Oligocene–Late Miocene lacustrine systems of the north-central part of the Ebro Basin (Spain): sedimentary facies model and palaegeographic synthesis. Palaeogeography, Palaeoclimatology and Palaeoecology 151, 127–48.

Arlegui, L.E., Soriano, M.A., 1998. Characterizing lineaments from satellite images and field studies in the central Ebro basin (NE Spain). International Journal of Remote Sensing 19(16), 3169–3185.

Artieda, O., Herrero, J., Drohan, P.J., 2006. Refinement of the differential water loss method for gypsum determination in soils. Soil Science Society of America Journal 70, 1932–1935.

Badía, D., Martí, C., Casanova, J., Gillot, T., Cuchí, J.A., Palacio, J., Andrés, R., 2015. A Quaternary soil chronosequence study on the terraces of the Alcanadre River (semiarid Ebro Basin, NE Spain). Geoderma 241-242, 158–167.

Bartolomé, M., Sancho, C., Moreno, A., Oliva-Urcia, B., Belmonte, A., Bastida, J., Cheng, H., Edwards, R.L., 2015. Upper Pleistocene interstratal piping-cave

speleogenesis: The Seso Cave System (Central Pyrenees, Northern Spain). Geomorphology 228, 335–344.

Batalla. R.J., Balasch, J.C., 2001. Interpretación hidrodinámica y sedimentaria de la rotura de la balsa de San Juan (Altorricón, Huesca). Cuaternario y Geomorfología 15(3-4), 109-123.

Bayly, I.A.E., Williams, W.D., 1973. Inland waters and their ecology. Longman, Camberwell, 316 pp.

Bomer, B., 1979. Les piedmonts du Bassin de l'Ebre (Espagne). Mediterranée 3, 19-25.

Bryan, R., Yair, A. (Eds.), 1982. Badland geomorphology and piping. GeoBooks, Norwich, UK, 408 pp.

Bridge, J.S., 2003. Rivers and floodplains; Forms, Processes and Sedimentary Record. Blackwell Science Ltd., Oxford, 491 pp.

Bridge, J.S, Demicco, R.V., 2008. Earth surface processes, landforms and sediment deposits. Cambridge University Press, Cambridge, UK. 815 pp.

Calle, M., Sancho, C., Peña, J.L., Cunha, P., Oliva-Urcia, B., Pueyo, E., 2013. La secuencia de terrazas cuaternarias del río Alcanadre (provincia de Huesca): Caracterización y consideraciones paleoambientales. Cuadernos de Investigación Geográfica 39(1), 159–178.

CBDSA (Comisión del Banco de Datos de Suelos y Aguas). 1983. SINEDARES. Manual para la Descripción Codificada de Suelos en el Campo. Ministerio de Agricultura, Pesca y Alimentación, Madrid, 137 pp. Available at http://www.iec.cat/mapasols/DocuInteres/PDF/Llibre12.pdf, accessed on 20-02-2017.

Coleman, J., 1969. Brahmaputra River: channel processes and sedimentation. Sedimentary Geology 3, 129–239.

Costa, J.M., Ramírez Merino, J.I., Navarro, J.J., Salazar, A., Simón, J.L., Hernández Samaniego, A., Del Olmo, A., Ramírez del Pozo, J., Cuenca Bescós, G., Barnolas, A., Robador, A., 1998. Memoria y mapa geológico de España E. 1:50.000, Sheet no. 356, Lanaja. Instituto Tecnológico GeoMinero de España, Madrid, 65 pp. + 2 maps. Available at http://info.igme.es/cartografia/magna50.asp?hoja=356, accessed on 20-02-2017.

Cuchí, J.A., Andrés, R., Badía, D., Martí, C., 2012. Notas sobre ventifactos en la cuenca baja del río Alcanadre (Sariñena, Huesca). Lucas Mallada 14, 187-192. Available at https://dialnet.unirioja.es/ejemplar/396032, accessed on 20-02-2017.

Dahlin, T., Zhou, B., 2004. A numerical comparison of 2D resistivity imaging with 10 electrode arrays. Geophysical Prospecting 52, 379–398.

Dantin, J., 1942. Distribución y extensión del endorreísmo aragonés. Estudios Geográficos 8, 505-596.

Darmendrail, D., Cerdan, O., Gobin, A., Blanchard, B., Siegele, B., 2004. Assessing the Economic Impacts of Soil Degradation. Case Studies and Database Research. BRGM RP 53091. Available at http://ecologic.eu/1006, accessed on 20-02-2017.

Davis, W.M., 1882. On the classification of lake basins. Proceedings of the Boston Society of Natural History 21, 315–381.

Desir, G., Marín, C., 2011. Influencia de los procesos de piping en la evolución del modelado, Bardenas Reales (Navarra, España). Cuadernos de Investigación Geográfica 37, 67–78.

Desir, G., Gutiérrez-Elorza, M., Gutiérrez-Santolalla, F., Marín, C., 2011. Las formas y depósitos eólicos de la Depresión del Ebro. In: E. Sanjaume and F.J. Gracia (Editors.). Las dunas en España. S.E.G., Cádiz, pp. 563–581.

Duval, M., Sancho, C., Calle, M., Guilarte, V., 2015. On the interest of using the multiple center approach in ESR dating of optically bleached quartz grains: Some examples from the Early Pleistocene terraces of the Alcanadre River (Ebro basin, Spain). Quaternary Geochronology 29, 58–69.

Eberhard, R., Sharples, C., 2013. Appropriate terminology for karst-like phenomena: the problem with "pseudokarst". International Journal of Speleology 42(2), 109–113.

Faci, J., Martínez-Cob, A., 1991. Cálculo de la evapotranspiración de referencia en Aragón. Departamento de Agricultura. Gobierno de Aragón, pp. 115. Available at http://hdl.handle.net/10261/73507, accessed on 20-02-2017.

Faulkner, H., Spivey, D., Alexander, R., 2000. The role of some site geochemical processes in the development and stabilisation of three badland sites in Almeria, southern Spain. Geomophology 35, 87–99.

García-González, M.T., Wierzchos, J., Vizcayno, C., Rodríguez, R., 1996. Fine-Grained laminated quaternary sediments in the Ebro Valley (Spain): characteristics and formation. Clay Minerals 31, 173–181.

García-Ruiz, J.M., 2011 Una revisión de los procesos de sufosión o *piping* en España. Cuadernos de Investigación Geográfica 37(1), 7-24.

García-Ruiz, J.M., Lasanta, T., Alberto, F., 1997. Soil erosion by piping in irrigated fields. Geomorphology 30, 269–278.

Giampaolo, V., Capozzoli, L., Grimaldi, S., Rizzoa, E., 2016. Sinkhole risk assessment by ERT: The case study of Sirino Lake (Basilicata, Italy. Geomorphology 253, 1–9.

Goudie, A.S., 2013. Arid and semi-arid Geomorphology. Cambridge University Press, New York, 461 pp.

Gutiérrez-Elorza, M., 2005. Climate Geomorphology. Developments in Earth Surface Processes 8, 760 pp. Elsevier, Amsterdam.

Gutiérrez, M., Desir, G., Gutiérrez, F., 2002a. Yardangs in the semiarid central sector of the Ebro Depression (NE Spain). Geomorphology 44, 155–170.

Gutiérrez, F., Desir, G., Gutiérrez, M., 2002b. Causes of the catastrophic failure of an earth dam built on gypsiferous alluvium and dispersive clays (Altorricón, Huesca Province, NE Spain). Environmental Geology 43, 842–851.

Gutiérrez, M., Sancho, C., Benito, G., Sirvent, J., Desir, G., 1997. Quantitative study of piping processes in badland areas of the Ebro Basin, NE Spain. Geomorphology 20, 237–253.

Gutiérrez, F., Valero-Garcés, B., Desir, G., González-Sampériz, P., Gutiérrez, M., Linares, R., Zarroca, M., Moreno, A., Guerrero, J., Roqué, C., Arnold, L.J., Demuro, M., 2013. Late Holocene evolution of playa lakes in the central Ebro depression based on geophysical surveys and morpho-stratigraphic analysis of lacustrine terraces. Geomorphology 196, 177–197.

Hakanson, L., 2007. Lake environments. In: C. Perry, K. Taylor (Eds.), Environmental sedimentology, Blackwell Publishing, Malden (USA), pp 109–143.

Harvey, A.M., 1982. The role of piping in the development of badlands and gully systems in south-east Spain. In R. Bryan, Yair, A. (Eds.): Badland geomorphology and piping 3, 17–336.

Harvey, A.M., Gutiérrez-Elorza, M., 2005. Repeated patterns of Quaternary discontinuous gullying at El Tormillo, Ebro Basin, Spain. In C. García & R.J. Batalla (Eds.): Catchment Dynamics and River Processes: Mediterranean and Other Climate Regions. Elsevier, pp. 53–67.

Heanes, D.L., 1984. Determination of total organic-C in soils by an improved chromic acid digestion and spectrophotometric procedure. Commun. Soil Sci. Plant Anal. 15, 1191–1213.

Hernández Samaniego, A., Salazar, A., Del Olmo, A., Navarro, J.J., Simón, J.L., Rodríguez Santistéban, R., Almoguera, F.J., García Villar, A, Barnolas, A., Robador, A., 1998. Memoria y mapa geológico de España E. 1:50.000, Sheet no. 357, Sariñena. Instituto Tecnológico GeoMinero de España, Madrid, 57 pp. + 2 maps. Available at http://info.igme.es/cartografia/magna50.asp?hoja=357. accessed on 20-02-2017.

Herrero, J., Rodríguez-Ochoa, R., Porta, J. 1989. Colmatación de drenes en suelos afectados por salinidad. Instituto Fernando el Católico. Zaragoza, Spain, 134 pp. Available at http://ifc.dpz.es/recursos/publicaciones/15/82/_ebook.pdf, accessed on 20-02-2017.

Higgins, C.G., Schoner, C., 1997. Sinkholes formed by piping into buried channels. Geomorphology 20, 307–312.

Huddart, D., Bennett, M.R., 2000. Subsidence structures associated with subaerial desiccation-crack piping and their role in drainage evolution on a drained proglacial lake bed: Hagavatn, Iceland. Journal of Sedimentary Research 70(5), 985–993.

Hutchinson, G.E., 1957. A Treatise on Limnology. Vol. 1. John Wiley and Sons, New York, 1015 pp.

Ibáñez, M.J., 1975. El endorreísmo del sector central de la Depresión del Ebro. Cuadernos de Investigación (Geografía e Historia) 1(2), 35–48.

Ibáñez, M.J., Pellicer, F., Echeverría, M.T., 1984. Notas geomorfológicas sobre la Laguna de Sariñena. Geographicalia 21-24, 25–41.

Jones, J.J.A., 1981. The nature of de soil piping: A review of the research. British Geomorphological Research Group Monograph Series 3. Geobooks. 301 pp. Norwich.

Jones, J.J.A., 1994. Soil piping and its hydrogeomorphic function. Cuaternario y Geomorfología 8(3–4), 77–102.

Jones, J.J.A., 2004. Pipe and piping. In: A.S. Goudie (Ed.), Encyclopedia of Geomorphology, Routeledge, London, pp. 784–788.

Khobzy, J., 1972. Érosion chimique et mécanique dans la genèse de dépressions «pseudokarstiques» souvent endoréiques. Revue de Géomorphologie Dynamique 2, 2–69.

Lebrón, I., 1988. Suelos salino-sódico-alcalinos de la Depresión media del Ebro. Condiciones de formación, características y propiedades. PhD Thesis, Zaragoza, 483 pp. Available at http://hdl.handle.net/10261/78378, accessed on 20-02-2017.

Lees, B.G., Cook, P.G., 1991. A conceptual model of lake barrier and compound lunette formation. Palaeogeography, Palaeoclimatology, Palaeocology 84, 271–284.

Lewis, C., McDonald, E., Sancho, C., Peña, J.L., Rhodes, E., 2009. Climatic implications of correlated Upper Pleistocene glacial and fluvial deposits on the Cinca and Gállego Rivers (NE Spain) base on OSL dating and soil stratigraphy. Global and Planetary Change 67, 141–152.

Li, J., Bristow, C.S., 2015. Crevasse splay morphodynamics in a dryland river terminus: Río Colorado in Salar de Uyuni Bolivia. Quaternary International 377, 71–82

Loperte, A., Soldovieri, F., Palombo, A., Santinia, F., Lapenna, V., 2016. An integrated geophysical approach for water infiltration detection and characterization at Monte Cotugno rock-fill dam (southern Italy) Engineering Geology 211, 162–170.

Luzón, A., 2005. Oligocene-Miocene alluvial sedimentation in the northern Ebro Basin, NE Spain: Tectonic control and palaeogeographical evolution. Sedimentary Geology 117, 19–39.

Luzón, A., González, A., Muñoz, A., Sánchez-Valverde, B., 2002. Upper Oligocene–Lower Miocene shallowing upward lacustrine sequences controlled by periodic and non-periodic processes (Ebro Basin, Spain). Journal of Paleolimnology 28, 441–6.

MAPA, 1994. Métodos oficiales de análisis. Tomo III. Ministerio de Agricultura, Pesca y Alimentación. Madrid, 662 pp.

Martínez-Cob, A., Zapata, N., Sánchez, I., 2010. Viento y riego. La variabilidad del viento en Aragón y su influencia en el riego por aspersión. Institución Fernando El Católico, Zaragoza, Spain, 200 pp. Available at http://digital.csic.es/handle/10261/23680, accessed on 20-02-2017.

Martínez-Pagán, P., Gómez-Ortiz, D., Martín-Crespo, T., Manteca, J.I., Rosique, M., 2013. The electrical resistivity tomography method in the detection of shallow mining cavities. A case study on the Victoria Cave, Cartagena (SE Spain). Engineering Geology 156, 1–10.

Mensua, S., Ibáñez, M.J., 1977. Terrazas y glacis del centro de la Depresión del Ebro. III Reunión Nacional Grupo de Trabajo del Cuaternario, Madrid, pp. 23–41.

Mingarro, F., Ordóñez, S., López de Azcona, M.C., García del Cura, M.A., 1981. Sedimentoquímica de las lagunas de los Monegros y su entorno geológico. Boletín Geológico y Minero 92-93, 171–195.

Mjos, R., Walderhaug, O., Prestholm, E., 1993. Crevasse splay sandstone geometries in the Middle Jurassic Ravenscar Group of Yorkshire, UK. Spec. Publ. int. Ass. Sediment. 17, 167–184.

Montes, L., Domingo, R., Peña-Monné, J.L., Sampietro-Vattuone, M.M., Rodríguez-Ochoa, R., Utrilla, P., 2016. Lithic materials in high fluvial terraces of the central Pyrenean piedmont (Ebro Basin, Spain). Quaternary International 393, 70–82.

Otvos, E.G., 1976. "Pseudokarst" and "pseudokarst terrains": Problems of terminology. Geological Society of America Bulletin 87(7), 1021.

Parker Sr, G.G., Higgins, C.G., Wood, W.W., 1990. Piping and pseudokarst in drylands. In: C.G. Higgins & D.R. Coates (Eds.), Groundwater Geomorphology: the role of subsurface water in earth-surface processes and landforms. Special Paper 252. The Geological Society of America, Boulder, Colorado, pp. 77–110.

Pontén, A., Plink-Björklund, P., 2007. Depositional environments in an extensive tide-influenced delta plain, Middle Devonian Gauja Formation, Devonian Baltic Basin. Sedimentology 54, 969–1006.

Pratdesaba, E., 1997. Processos d'erosió en galeries de parcelles abancalades del sistema de regadius Flumen-Monegros. Escola Tecnica Superior d'Enginyeria Agriaria (ETSEA), University of Lleida, Spain, 180 pp.

Quinlan, J.F., 1966. Classification of karst and pseudokarst types. Geological Society of America, Special Paper 101, 448–450.

Quirantes, J., 1965. Nota sobre las lagunas de Bujaraloz-Sástago. Geographica 12, 30–34.

Quirantes, J., 1978. Estudio sedimentológico y estratigráfico del Terciario continental de Los Monegros. CSIC, Institución Fernando el Católico, Zaragoza, 117 pp.

Reeves Jr., C.C., 1968. Introduction to Paleolimnology. Elsevier, Amsterdam, 228 pp.

Riba, O., Reguant, S., Villena, J., 1983. Ensayo de síntesis estratigráfica y evolutiva de la Cuenca terciaria del Ebro. In: Libro Jubilar J.M. Ríos, Geología de España. Instituto Geológico y Minero de España, Madrid, Vol. 2, pp. 131–159.

Rodríguez, V., Gutierrez, F., Green, A.G., Carbonel, D., Horstmeyer, H., Schmelzbach, C., 2014. Characterizing Sagging and Collapse Sinkholes in a Mantled Karst by Means of Ground Penetrating Radar (GPR). Environmental & Engineering Geoscience 20(2), 109–132.

Rodríguez-Ochoa, R., Herrero, J., Porta, J., 1989. Suelos de regadío con drenaje enterrado. XVI Reunión de la Sociedad Española de la Ciencia del Suelo. Guía de las excursiones. Lleida, Spain, 95 pp.

Rodríguez-Ochoa, R., Herrero, J., Porta, J., 1990. Micromorphological assessment of drain siltation risk indexes in a saline-sodic soil in Monegros irrigation District (Spain). In: L.A. Douglas (Ed.). Soil Micromorphology: a Basic and Applied Science. Elsevier, Amsterdam, pp. 41–52.

Rodríguez-Ochoa, R., Artieda, O., 1999. Introducción a los suelos de Monegros. Boletin Sociedad Entomológica Aragonesa (SEA) 24, 67–72.

Rodríguez-Ochoa, R., Pratdesaba, E., Olarieta, J.R., Sanchez, J., 1999. Gully piping erosion processes and structural instability of salt-affected soils (Flumen-Monegros area, Spain). In: J. Bech (Ed.). Sixth international Meeting on Soils with Mediterranean Type of Climate, Barcelona, Spain, pp 1045–1047. Publicacions Universitat de Barcelona.

Rodríguez-Ochoa, R., Olarieta, J.R., Domingo, F., Nogués, J., 2000. Irrigated soilscapes in the Flumen-Monegros district: productivity, soil processes, and environmental impacts. pp. 80–130. In: J. Boixadera, RM. Poch and C. Herrero (Eds.). Soilscapes of Catalonia and Aragon (NE Spain): Tour guide of the annual excursion of the Belgian Soil Science Society 1999. Société Belge de Pédologie.

Rodríguez-Vidal, J., 1986. Geomorfología de las Sierras Exteriores oscenses y su piedemonte. Colección de Estudios Altoaragoneses 4, Huesca, 172 pp.

Romero-Díaz, A., Marín Sanleandro, P., Sánchez Soriano, A., Belmonte Serrato, F., Faulkner, H., 2007. The causes of piping in a set of abandoned agricultural terraces in southeast Spain. Catena 69, 282–293.

Sánchez, J.A., Pérez, A., Coloma, P., Martínez Gil, J., 1998. Combined effects of groundwater and aeolian processes in the formation of the northernmost closed saline depressions of Europe: north-east Spain. Hydrological Processes 12, 813–820.

Sancho, C., Peña, J.L., Belmonte, A., Souza, V., Fort, R., Longares, L.A., Sopena, M.C., 2004. El modelado en areniscas de Los Torrollones de Gabarda (Monegros, Huesca). In: J.L. Peña, L.A. Longares and M. Sánchez (Eds.). Geografía física de Aragón. Aspectos generales y temáticos. Univ. Zaragoza & Institución Fernando el Católico, Zaragoza, pp. 329–343.

Sancho, C., Calle, M., Peña-Monné, J.L., Duval, M., Oliva-Urcia, B., Pueyo, E.L., Benito, G., Moreno, A., 2016. Dating the Earliest Pleistocene alluvial terrace of the Alcanadre River (Ebro Basin, NE Spain): Insights into the landscape evolution and involved processes. Quaternary International 407, 86–95.

Schoeneberger, P.J., Wysocki, D.A., Benham, E.C., Soil Survey Staff, 2012. Field book for describing and sampling soils. Version 3.0. Natural Resources Conservation Service. National Soil Survey Center, Lincoln, NE. Available at http://www.nrcs.usda.gov/wps/portal/nrcs/detail/soils/ref/?cid=nrcs142p2_054184 , accessed on 20-02-2017.

Selby, M.J., 1982. Hillslope Materials and Processes. Oxford University Press, New York, 264 pp.

Semeniuk, C.A., Semeniuk, V. 1995. A geomorphic approach to global classification for inland wetlands. Vegetatio 118, 103–124.

Shaw, P., Bryant, R., 2011. Pans, playas and salt lakes. In: D. Thomas (Ed.), Arid Zone Geomorphology, John Wiley and Sons, 373–401.

Sirvent, J., Desir, G., Gutiérrez, M., Sancho, C., Benito, G. 1997. Erosion rates in badland areas recorded by collectors, erosion pins and profilometer techniques (Ebro Basin, NE-Spain). Geomorphology 18, 61–75.

Smith, N.D., Cross, T.A., Dufficy, J.P., Clough, S.R., 1989. Anatomy of an avulsion. Sedimentology 36, 1–23.

Soil Survey Division Staff, 1993. Soil survey manual. Natural Resources Conservation Service, Handbook 18. USDA, Washington, DC.

Soil Survey Staff (SSS), 2014. Keys to Soil Taxonomy. 12th ed. USDA - Natural Resources Conservation Service, Washington DC., 360 pp. Available at http://www.nrcs.usda.gov/wps/portal/nrcs/detail/soils/survey/class/?cid=nrcs142p2_053580, accessed on 20-02-2017.

Stange, K.M., Van Balen, R.T., Carcaillet, J., Vandenberghe, J., 2013. Terrace staircase development in the southern Pyrenees foreland: inferences from 10Be terrace exposure ages at the Segre River. Global and Planetary Change 101, 97–112.

Stange, K.M., Van Balen, R.T., García-Castellano, D., Cloetingh, S., 2016. Numerical modelling of Quaternary terrace staircase formation in the Ebro foreland basin, southern Pyrenees, NE Iberia. Basin Research 28, 124–146.

Taubner, H., Roth, B., Tippkotter, R., 2009. Determination of soil texture: comparison of the sedimentation method and the laser-diffraction analysis. Journal of Plant Nutrition and Soil Science 172, 161–171.

Ternam, J.L., Elmes, A., Fitzjohn, C., Williams, A. G., 1998. Piping susceptibility and the role of hydro-geomorphic controls in pipe development in alluvial sediments, Central Spain. Zeitschrift für Geomorphologie 42(1), 75–87.

Timms, B.V., 1992. Lake Geomorphology. Gleneagles Publ., Adelaide, 180 pp.

United States Salinity Laboratory Staff, 1954. Diagnosis and improvement of saline and alkali soils. Agriculture Handbook No. 60. USDA (Reprinted 1969).

Valero-Garcés, B.L., González-Sampériz, P., Navas, A., Machín, J., Delgado-Huertas, A., Peña-Monné, J.L., Sancho-Marcén, C., Stevenson, T., Davis, B. 2004. Paleohydrological fluctuations and steppe vegetation during the last glacial maximum in the central Ebro valley (NE Spain). Quaternary International 122, 43–55.

Van Reeuwijk, L.P., 2002. Procedures for Soil Analysis. sixth ed. ISRIC-FAO. International Soil Reference and Information Centre, Wageningen (The Nertherlands), 120 pp.

Van Toorenenburg, K.A., Donselaar, M.E., Noordijk, N.A., Weltje, G.J., 2016. On the origin of crevasse-splay amalgamation in the Huesca fluvial fan (Ebro Basin, Spain): Implications for connectivity in low net-to-gross fluvial deposits. Sedimentary Geology 343, 156–164.

Vizcayno, C., García-González, M.T., Gutiérrez, M., Rodríguez, R., 1995. Mineralogical, chemical and morphological features of salt accumulations in the Flumen-Monegros district, NE Spain. Geoderma 68, 193–210.

Wood, W.W., Osterkamp, W.R., 1987. Playa-lake basins on the Southern High Plains of Texas and New Mexico: Part II. A hydrologic model and mass-balance arguments for their development. Geological Society of America Bulletin 99(2), 224-230.

Wright, H.E. Jr., 1964. Origin of the lakes in the Chuska Mountains, Northwestern New Mexico. Geological Society of America Bulletin 75, 589–598.

Zeng, R.Q., Meng, X.M., Zhang, F.Y., Wang, S.Y., Cui, Z.J., Zhang, M.S., Zhang, Y., Chen, G., 2016. Characterizing hydrological processes on loess slopes using

electrical resistivity tomography. A case study of the Heifangtai Terrace, Northwest China. Journal of Hydrology 541, 742–753.

Table 1. Pediment and fluvial terrace levels in the Alcanadre, Flumen and Cinca rivers (Costa et al., 1998; Hernández Samaniego et al., 1998).

Pediment levels	Alcanadre River	Flumen River	Cinca River
	Pyrenean piedmont high level (+ 180 m)		
P5	T6 (+ 60-100 m)		
P4	T5 (+ 65-70 m)		
P3	T4 (+ 35-60 m)	T3 (+ 35-40 m)	T3 (+ 30-40 m)
P2	T3 (+ 20-30 m)	T2 (+ 20-25 m)	
P1	T2 (+ 15 m)		T2 (+ 15 m)
	T1 (+ 10 m)	T1 (+ 10 m)	T1 (+ 10 m)

Table 2. The Alcanadre River terrace levels and their estimated ages (Calle et al., 2013).

Terrace level	Absolute height m a.s.l.	Relative height m	Estimated age kyr
T1	420	160-200	1276
T2	---	100	1000 – 780
T3	325	55	780
T4	300	30	< 780
T5	270	20-25	44
T6	---	25	19
T7	260	10	10
T8	255	3-5	---
T9	250	Present floodplain	

Table 3. LiDAR-derived height of the fluvial terrace levels (T) in the Alcanadre-Flumen River system and the lacustrine pediment-terraces (PT) of the Sariñena Basin.

Terraces in Alcanadre-Flumen River system				**Pediment-terraces in Sariñena basin**		
Level	Relative* height	Height range	Standard deviation	Level	Height above the lake bottom	Height above the Alcanadre River thalweg
	m				m	
T7	63.1	27.4	10.7			
T6	45.1	3.8	1.7			
T5	40.9	11.8	4.3	PT3	9-13	33-37
T4	32.9	9.6	4.4	PT2	4-7	28-31
T3	25.1	10.8	3.9	PT1	2-3	24-27
T2	13.9	4.9	1.6			
T1	8.6	4.7	2.0			

Table 4. Selected soil data for pedons representative of the main geomorphic units in the Sariñena lacustrine basin (pHp: pH measured in the saturated soil paste; CEe: electrical conductivity of the saturated soil-paste extract; OM: organic matter; CCE: calcium carbonate equivalent; SAR: sodium absorption ratio).

Horizons	Depth cm	pHp	CEe dS m^{-1} 25ºC	OM	CCE	Sand	Silt	Clay	USDA textural class	SAR
						%				
Pediment-Terrace 3/LN-1/Typic Natrixeralf										
Ap	0-22	8.3	8.08	0.82	17.0	30.6	31.3	38.1	Clay loam	16.8
Btn	22-40	8.3	3.72	0.85	17.0	37.9	29.3	32.8	Clay loam	11.2
Btnk	40-110	8.6	2.41	0.61	30.0	34.3	33.2	32.6	Clay loam	4.6
2C (lutite)	> 110	---	---		---	---		---	---	---
Pediment-Terrace 2/LO-21/Calcic Haploxerept										
A	0-23	8.2	2.19	1.48	24.0	19.7	27.6	52.6	Clay loam	3.6
Bwk	23-74	8.3	8.02	0.59	31.0	26.7	34.0	39.3	Loam	18.2
2Bwk	74-110	8.2	29.70	0.33	32.0	24.5	32.7	42.8	Loam	39.7
2CB	> 110	---	---		---	---		---	---	---
Pediment-Terrace 1/LO-7/Calcic Haploxerept										
Ap	0-27	8.7	2.05	1.34	22.2	49.5	28.3	22.2	Loam	5.3
Bwkg	27-93	9.1	2.17	0.57	25.5	52.9	21.6	25.5	Silt loam	6.9
2C (lutite)										
High slope (40%)/LO-3/Xeric Torriorthent										
A	0-32	8.2	2.23	2.87	30.0	21.3	43.2	35. 5	Loam	4.4
2C (lutite)	32-53	---	---		---	---		---	---	---
Low slope (5%)/LO-6/Typic Xerorthent										
A1	0-20	8.5	1.49	0.92	30.0	21.	42.9	36.1	Loam	3.3
A2	20-40	8.7	5.46	0.66	33.0	25.4	50.2	24.4	Silt loam	14.4
Bwy	40-68	8.2	2.97	0.17	6.0	26.6	69.6	3.8	Silt loam	1.8
2Cy (lutite)	68-80	---	---		---	---		---	---	---
Palustrine depression/FL-4/Sodic Calcixerept										
Ag	0-18	7.9	4.66	1.27	23.4	45.7	39.2	15.1	Clay	14.9
Bwg1	18-35	8.3	5.39	2.47	16.9	55.4	38.1	6.5	Clay	19.6
Bwg2	35-60	8.6	5.62	0.91	12.3	54.4	34.8	10.8	Clay	21.3
Bwkg1	60-95	8.7	6.73	0.71	24.1	59.1	33.0	8.0	Clay	22.8
Bwkg2	95-120	8.5	7.91	0.63	33.0	53.0	35.2	11.8	Clay	25.4
2C	120-160	8.5	7.91	0.52	30.5	45.9	32.5	11.8	Clay	25.4

Table 5. Selected characteristics of the claystones and sandstones in the Sariñena lacustrine basin (Locations shown in Fig. 7). CCE: calcium carbonate equivalent; Gyp: gypsum; pHp: pH measured in the saturated soil paste; CEe: electrical conductivity of the saturated soil-paste extract; SAR: sodium absorption ratio.

Sample	Sand	Silt	Clay	CCE	Gyp	pHp	CEe	SAR	Clay minerals of oriented aggregates, %		
	%						dS m^{-1} 25 ºC		Quartz	Calcite	Illite
Lutites											
LAG-1	2.2	58.1	39.7	18.6	0	8.5	12.9	29.5	4	17	76
LAG-2	4.1	52.0	43.9	24.1	0	9.1	8.1	33.3			
LAG-4	3.9	47.6	48.5	24.7	0	8.6	18.6	49.2			
CP-21	5.9	53.2	40.8	12.3	0	8.3	12.2	29.4	8	13	71
Sandstones											
AR-1a	70.9	21.0	8.1	28.2	0						
AR-1b	54.4	39.0	6.7	32.8	0						
AR-2a	88.8	7.2	4.1	16.8	0						
AR-2b	79.9	12.2	8.0	15.5	14.3						

Highlights

- A genetic model is proposed for Sariñena Lake which involves piping processes.
- Data from photointerpretation, LiDAR, soils, and geophysics were used for reconstructing lake origin and evolution.
- A new type of lakes is proposed, generated by the removal of subsurface materials, including karst-related lakes and those formed by piping processes